

On the singular Neumann problem in linear elasticity

Miroslav Kuchta¹  | Kent-Andre Mardal^{1,2}  | Mikael Mortensen¹ 

¹Department of Mathematics, Division of Mechanics, University of Oslo, Blindern 0316 Oslo, Norway

²Department of Computational Physiology, Simula Research Laboratory, Martin Linges Vei 25 1364 Fornebu, Norway

Correspondence

Miroslav Kuchta, Department of Mathematics, Division of Mechanics, University of Oslo, Blindern, 0316 Oslo, Norway.
Email: mirok@math.uio.no

Funding information

Research Council of Norway, Grant/Award Number: 179578

Summary

The Neumann problem of linear elasticity is singular with a kernel formed by the rigid motions of the body. There are several tricks that are commonly used to obtain a nonsingular linear system. However, they often cause reduced accuracy or lead to poor convergence of the iterative solvers. In this paper, different well-posed formulations of the problem are studied through discretization by the finite element method, and preconditioning strategies based on operator preconditioning are discussed. For each formulation, we derive preconditioners that are independent of the discretization parameter. Preconditioners that are robust with respect to the first Lamé constant are constructed for the pure displacement formulations, whereas a preconditioner that is robust in both Lamé constants is constructed for the mixed formulation. It is shown that, for convergence in the first Sobolev norm, it is crucial to respect the orthogonality constraint derived from the continuous problem. On the basis of this observation, a modification to the conjugate gradient method is proposed, which achieves optimal error convergence of the computed solution.

KEYWORDS

conjugate gradient, linear elasticity, preconditioning, rigid motions, singular problems

1 | INTRODUCTION

This paper discusses numerical techniques for solving the singular problem of linear elasticity. Let $\Omega \subset \mathbb{R}^3$ be the body subjected to volume forces $f : \Omega \rightarrow \mathbb{R}^3$ and surface forces $h : \partial\Omega \rightarrow \mathbb{R}^3$. The body's displacement $u : \Omega \rightarrow \mathbb{R}^3$ is then found as a solution to

$$\begin{aligned} -\nabla \cdot \sigma(u) &= f && \text{in } \Omega, \\ \sigma(u) &= 2\mu\epsilon(u) + \lambda(\nabla \cdot u)I && \text{in } \Omega, \\ \sigma(u) \cdot n &= h && \text{on } \Gamma_N = \partial\Omega, \end{aligned} \quad (1)$$

with $\mu > 0$ and $\lambda \geq 0$ as the Lamé constants of the material, I as the identity matrix, $\epsilon(u) = \frac{1}{2}(\nabla u + (\nabla u)^\top)$ as the strain, and n as the outward-pointing surface normal (see the work of Marsden and Hughes¹). We note that the constitutive law for the stress tensor σ can be equivalently stated as $\sigma(u) = 2\mu\epsilon(u) + \lambda\text{tr}(\epsilon(u))I$, where $\text{tr}(\epsilon(u))$ denotes the trace of $\epsilon(u)$, that is, the sum of its diagonal.

The system is used extensively in structural analysis² and is relevant in numerous applications, for example, marine engineering,³ biomechanics of brain,⁴ spine,⁵ or the mechanics of planetary bodies.⁶

Due to the absence of a Dirichlet boundary condition that can anchor the body (coordinate system) in space, the solution can be uniquely determined if and only if the net force and the net torque on Ω are zero, that is, the forces f and h satisfy

the compatibility conditions

$$\begin{aligned} \int_{\Omega} f \, dx + \int_{\partial\Omega} h \, ds &= 0, \\ \int_{\Omega} f \times x \, dx + \int_{\partial\Omega} h \times x \, ds &= 0. \end{aligned} \quad (2)$$

With such compatible data, the now solvable (1) is singular as any rigid motion can be added to the solution. We note that the space of rigid motions $z : \Omega \rightarrow \mathbb{R}^3$ such that $\epsilon(z) = 0$ consists of translations and rigid rotations, and for a body in 3D, the space is six-dimensional.

The ambiguity of the solution of (1) can be removed by adding constraints by means of Lagrange multipliers that enforce that the solution is free of rigid motions. When discretized, this approach yields an invertible saddle-point system. Alternatively, discretizing (1) directly leads to a symmetric, positive semidefinite matrix with a six-dimensional kernel. Singular systems may be solved by iterative methods if care is taken to handle the kernel during the iterations, but a common approach (here termed *pinpointing*) in the engineering literature (see, e.g., the DNV GL class guideline³) is to remove the null space by prescribing the displacement in selected points of $\partial\Omega$.

If $\Gamma_N \neq \partial\Omega$ and a Dirichlet boundary condition is prescribed on $\partial\Omega \setminus \Gamma_N$, the equations of linear elasticity are well-posed (see, e.g., chapter 6.3 in the work of Braess⁷), and there exists a number of efficient solution algorithms for the problem. Here, we discuss some of the methods for which the Neumann problem (1), or, more precisely, the correct treatment of the rigid motions, is relevant.

In the context of algebraic multigrid (AMG), it is recognized already in the early work of Ruge and Stüben⁸ that carefully constructed interpolators are needed to obtain good convergence for problems stemming from equations of linear elasticity (partial differential equation systems in general). In particular, the authors observe that with the so-called “unknown” approach convergence of AMG deteriorates when the number of Dirichlet boundaries decreases. The issue here is that with the “unknown” approach, only the translations are interpolated well on the coarse grid (cf. the work of Baker et al.⁹), and as a remedy, the authors propose to improve the interpolation of rotations (eigenvectors with small eigenvalues in general). Griebel et al.¹⁰ construct a block interpolation where the rotations are captured exactly if the underlying grid is point symmetric. However, this assumption fails to hold at the boundary nodes, and AMG becomes less effective as the number of Neumann boundaries increases. More recently, Baker et al.⁹ discusses computationally efficient techniques for augmenting a given/existing AMG interpolator to ensure an exact interpolation of rigid motions (null space vectors in general). A related approach is that by Vassilevski and Zikatanov,¹¹ who derive algorithms for constructing AMG interpolation operators that exactly interpolate any given set of vectors. The requirement that the coarse space captures rigid motions is also found in the later variants of AMG. For example, in smoothed aggregation AMG,^{12,13} the coarse basis functions are constructed from a (global) constrained minimization problem where preservation of the null space is one of the constraints. The minimization problems solved in the construction of AMG based on element interpolation^{14–16} use rigid motions of the local stiffness matrices. Similarly, the kernel of local stiffness matrices is preserved by the approximate splittings in AMG based on computational molecules.^{17,18}

Given that the restriction and interpolation operators preserve the kernel exactly and that the initial residual does not contain elements in the kernel, the singular problem at the coarsest level may be solved with Krylov methods, like the conjugate gradient (CG) method, which then work well. To complete our (nonexhaustive) list, let us mention that in the domain decomposition methods (e.g., finite element tearing and interconnecting¹⁹), the Neumann problem (1) arises naturally on “floating” subdomains that do not intersect the Dirichlet boundaries. Here, the local singular problem is treated algebraically by a pseudoinverse (cf. the discussion in Section 4).

In the following, we aim to solve (1) with the finite element method (FEM) while using Krylov methods for the resulting linear systems. As the systems are singular, the Krylov solvers are initialized with the null space of rigid motions (typically in the form of the l^2 orthonormal set of vectors). In the standard implementation,* the Krylov methods employ the same (l^2) projection to orthogonalize both the right-hand side as well as the solution vector with respect to the given null space. A particular question that we address here is then whether these algorithms provide discrete approximations that converge to the weak solution of (1) in the H^1 norm. We shall see that, in general, the answer is negative and that the issue stems from the fact that in the context of FEM, a vector in \mathbb{R}^n can be associated with a *function* from the finite-dimensional finite element space $V_h \subset H^1$, that is, it represents a solution/left-hand side, as well as with the *functional* from the

*See, for example, <http://www.mcs.anl.gov/petsc/petsc-current/docs/manualpages/KSP/KSPSolve.html>.

corresponding dual space, that is, it is a representation of the right-hand side. Consequently, two projectors are required in the iterative method originating from a singular variational problem. However, standard implementations of Krylov methods, which employ single projection, fail to make the distinction.

Rewriting the Krylov solvers to take the two representations into account is, in principle, a simple addition to the code. However, it is also intrusive in the sense that it requires modification of perhaps the low-level code in the implementation of the Krylov solvers. To the best of our knowledge, this distinction is not implemented in state-of-the-art linear algebra frameworks such as PETSc²⁰ or hypre.²¹ Here, we therefore propose a simple alternative solution that is less intrusive, although it requires a priori information about the kernel. Alternative methods, which require less or no a priori information, are the adaptive multigrid methods,^{22,23} where the null space is detected automatically during the solver setup in an iterative process that identifies error components that the current solver cannot effectively reduce. Here, we focus on the analysis of the Lagrange multiplier method and the CG method for the singular problem (1). Well-posedness of both the methods is discussed, and robust preconditioners are established based on operator preconditioning.²⁴ Further, connections between the two methods and the question of whether they yield identically converging numerical solutions are elucidated. These methods rely on standard iterative solvers as they implicitly contain the two required projectors.

This paper is structured as follows. In Section 2, the necessary notation is introduced, and shortcomings of pinpointing and CG are illustrated by numerical examples. Section 3 discusses Lagrange multiplier formulation and the two preconditioners for the method. Section 4 deals with the preconditioned CG method, and two preconditioners are proposed. Further, it is revealed that if the continuous origin of the discrete problem is ignored, the method, in general, will not yield convergent solutions. A continuous variational setting is introduced to modify the CG to yield a convergent method. Section 5 discusses well-posedness and preconditioning of an alternative formulation of (1). The proposed formulation leads to a symmetric, positive definite linear system. In Sections 3–5, we assume that λ and μ are of comparable magnitude in order to put the focus on the proper handling of the rigid motions. In Section 6, we consider the case where $\lambda \gg \mu$. The focus here is on a well-known and simple technique to remove the problems of locking, namely, the mixed formulation of linear elasticity where an extra unknown, the *solid pressure*, is introduced. We discuss two formulations that yield robust approximation and preconditioning in λ when care is taken in the proper handling of the rigid motions. Finally, conclusions are drawn in Section 7.

2 | PRELIMINARIES

Let V be the Sobolev space of vector-valued (or scalar or tensor) functions, which, together with their weak derivatives of order 1, are in space $L^2(\Omega)$. We denote by (\cdot, \cdot) the $L^2(\Omega)$ inner product of functions in V , whereas $\|\cdot\|$ is the corresponding norm. For the L^2 inner product over boundary $\partial\Omega$, we shall use the notation $(\cdot, \cdot)_{\partial\Omega}$. The standard inner product of V is $(u, v)_1 = (u, v) + (\nabla u, \nabla v)$, $u, v \in V$, and $\|\cdot\|_1$ shall be the induced norm. For any Hilbert space V , its dual space is denoted as V' , and we use capital or calligraphy letters to denote operators, for example, $A : V \rightarrow V'$ or $\mathcal{A} : (V \times V) \rightarrow (V \times V)'$. Finally, $\langle \cdot, \cdot \rangle$ is the duality pairing between V' and V .

The space \mathbb{R}^n is considered with the l^2 inner product $x^\top y = x_i y_i$ (invoking the summation convention), $x, y \in \mathbb{R}^n$ and the norm $|x| = \sqrt{x^\top x}$. For clarity of notation, bold fonts are used to denote vectors and operators (matrices) in \mathbb{R}^n that are representations of functions and operators from finite-dimensional finite element approximation space $V_h \subset V$. Let $\{\phi_i\}_{i=1}^n$ be the nodal basis of V_h . The representations are obtained by mappings $\pi_h : V_h \rightarrow \mathbb{R}^n$ (the nodal interpolant) and $\mu_h : V'_h \rightarrow \mathbb{R}^n$ such that for $v \in V_h$, $f \in V'_h$, we have

$$v = (\pi_h v)_i \phi_i \quad \text{and} \quad (\mu_h f)_i = \langle f, \phi_i \rangle. \quad (3)$$

We refer to chapter 6 in the work of Mardal and Winther²⁴ for a detailed discussion of the properties of the mappings, for example, invertibility, and note here that $M : V_h \rightarrow V'_h$ is represented by a matrix $\mathbf{M} = \mu_h M \pi_h^{-1}$. In particular, the mass matrix \mathbf{M} , $M_{ij} = (\phi_j, \phi_i)$ represents the Riesz map with respect to the L^2 inner product, $\langle Mu, v \rangle = (u, v)$, $u \in V_h$. On the other hand, the duality pairing between V'_h and V_h is represented by the l^2 inner product $\langle f, v \rangle = \mathbf{f}^\top \mathbf{v}$, $\mathbf{f} = \mu_h f$, $\mathbf{v} = \pi_h v$. We remark that for V_h set up on a sequence of nonuniformly refined triangulations of Ω , the l^2 inner product $\mathbf{u}^\top \mathbf{v}$, where $\mathbf{v} = \pi_h v$, $\mathbf{u} = \pi_h u$, may not provide a converging approximation of (u, v) , and the distinction between the two becomes crucial for the construction of converging methods.

TABLE 1 Convergence of the pinpointing approach for the singular Poisson problem

$d = 2$			$d = 3$		
Size	$\ u - u_h\ _1$	#	Size	$\ u - u_h\ _1$	#
40,849	2.49E-01 (1.00)	11	12,347	2.72E+00 (1.22)	10
162,593	1.25E-01 (1.00)	11	92,685	1.36E+00 (1.01)	11
648,769	6.23E-02 (1.00)	11	718,649	6.78E-01 (1.00)	12
2,591,873	3.11E-02 (1.00)	12	5,660,913	3.39E-01 (1.00)	12

Finally, Korn's inequalities on $V = [H^1(\Omega)]^3$ and $Z^\perp = \{v \in V; (v, z) = 0 \forall z \in Z\}$, $Z = \{v \in V; \epsilon(v) = 0\}$ are invoked (see Theorems 2.1 and 2.3 in the work of Ciarlet²⁵). There exists a positive constant $C = C(\Omega)$ such that

$$C\|u\|_1^2 \leq \|\epsilon(u)\|^2 + \|u\|^2 \quad \forall u \in V. \quad (4)$$

There exists a positive constant $C = C(\Omega)$ such that

$$C\|u\|_1^2 \leq \|\epsilon(u)\|^2 \quad \forall u \in Z^\perp. \quad (5)$$

To motivate our investigations and illustrate the lack of H^1 convergence that pinpointing or standard CG can lead to, we present three numerical examples. That pinpointing can be a suitable method for treating a singular problem is shown in the first example, which considers the Poisson problem with Neumann boundary conditions. However, pinpointing does not work well with (1) as the second example shows. In the third example, the singular elasticity problem is finally solved with a preconditioned CG.

Bochev and Lehoucq²⁶ report an increase in the iteration count due to pinpointing for a CG method without a preconditioner in the context of the singular Poisson problem. However, Krylov methods are, in practice, rarely applied without a preconditioner. For this reason, Example 1 solves the singular Poisson problem in two and three dimensions by means of pinpointing and a preconditioned CG.

Example 1. We consider $\Omega = [0, 1]^d$, $d = 2, 3$, and the singular Poisson equation

$$\begin{aligned} -\Delta u &= f && \text{in } \Omega, \\ \nabla u \cdot n &= 0 && \text{on } \partial\Omega, \end{aligned}$$

With the unique exact solution obtained by subtracting its mean value $|\Omega|^{-1} \int_\Omega u \, dx$ from a manufactured u . The value of the exact solution is prescribed as a constraint for the degree of freedom at the (bottom) lower-left corner of the domain, which is triangulated such that the computational mesh is refined toward the origin.

To discretize the system, continuous linear Lagrange elements[†] from the FEniCS library²⁷ were used. The resulting linear system was solved by the preconditioned CG method implemented in the PETSc library,²⁰ using hypreAMG²¹ to compute the action of the preconditioner. More specifically, we used a single V cycle with one pre- and postsmoothing by a symmetric successive over-relaxation smoother. The other AMG parameters were kept at their default settings, for example, *classical* interpolation and *Falgout* coarsening.[‡] The iterations were started from a random initial guess, and a relative preconditioned residual magnitude of 10^{-11} was required for convergence.

The number of iterations together with error and convergence rates based on the H^1 norm are reported in Table 1. Pinpointing yields numerical solutions u_h that converge at an optimal rate. Moreover, the number of iterations is bounded. Unlike in the work of Bochev and Lehoucq,²⁶ where specifying the solution datum in a single point was found to lead to an increasing number of *unpreconditioned* CG iterations (both in 2D and 3D), here, we find that a *preconditioned* CG with the system modified by pinpointing is a suitable numerical method for the singular Poisson problem.

Following the performance of pinpointing in the singular Poisson problem, the same approach is now applied to (1) in Example 2.

Example 2. We consider the singular elasticity problem (1) with $\mu = 384$, $\lambda = 577$, and Ω obtained by rigid deformation of the box $\left[-\frac{1}{4}, \frac{1}{4}\right] \times \left[-\frac{1}{2}, \frac{1}{2}\right] \times \left[-\frac{1}{8}, \frac{1}{8}\right]$. The box was first rotated around the x -, y -, and z -axes by angles $\frac{\pi}{2}$, $\frac{\pi}{4}$,

[†]Unless stated otherwise, continuous linear Lagrange elements (P_1) are used to discretize all the presented numerical examples.

[‡]The settings for AMG were reused throughout all the numerical experiments presented in this paper.

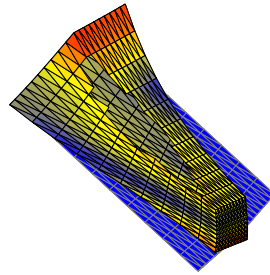


FIGURE 1 Computational domain (blue) deformed by exaggerated (4 \times) analytical displacement used in the numerical examples. The deformed body is colored by the magnitude of the displacement

TABLE 2 Convergence of the pinpointing approach for the singular elasticity problem

Size	3 \circ		1 \triangleright		3 \triangleright		3 \bullet	
	$\ u - u_h\ _1$	#	$\ u - u_h\ _1$	#	$\ u - u_h\ _1$	#	$\ u - u_h\ _1$	#
2187	6.69E-02 (-0.02)	30	1.01E-01 (-0.70)	32	2.82E-02 (0.88)	24	2.89E-02 (0.99)	25
14,739	1.27E-01 (-0.92)	35	9.61E-01 (-3.25)	40	1.08E-02 (1.38)	28	1.35E-02 (1.10)	29
107,811	2.57E-01 (-1.02)	36	7.89E+00 (-3.04)	48	1.72E-02 (-0.66)	31	1.08E-02 (0.31)	32
823,875	5.17E-01 (-1.01)	41	6.36E+01 (-3.01)	54	3.96E-02 (-1.21)	33	1.82E-02 (-0.75)	35

and $\frac{\pi}{5}$, respectively. Afterward, it was translated by the vector (0.1, 0.2, 0.3). Starting from $u^* = \frac{1}{4}(\sin \frac{\pi}{4}x, z^3, -y)$, the unique solution u of (1) is constructed by orthogonalizing u^* with respect to the rigid motions of Ω , where the orthogonality is enforced in the L^2 inner product, whereas the right-hand side f is manufactured by adding to $-\nabla \cdot \sigma(u)$ a linear combination of rigid motions. Finally, we take $\sigma(u) \cdot n$ as the surface force h . The solution is pictured in Figure 1. We note that, in this example, a uniform triangulation is used.

To obtain from (1) an invertible linear system, the exact displacement was prescribed in four different ways (cf. Table 2). (3 \circ) constrains six degrees of freedom in three corners of the body such that in the i th corner, there are i components prescribed. This choice is motivated by the dimensionality of the space of rigid motions (cf. the DNV GL class guideline³). The fact that fixing three points in space is sufficient to prevent the body from rigid motions motivates (1 \triangleright), where all three components of displacement are prescribed on vertices of a single triangular element on $\partial\Omega$. However, with mesh size decreasing, this constraint effectively becomes a constraint for a single point. Thus, in (3 \triangleright), the displacement in three arbitrary triangles is fixed. Finally, in (3 \bullet), the displacement is prescribed in three corners of the body.

The iterative solver used the same tolerances and parameters as in Example 1. In particular, identical settings of the multigrid preconditioner were utilized, and the iterations were started from a random initial vector. We note that AMG was *not* initialized with the rigid motions.

The number of iterations together with error and convergence rates based on the H^1 norm are reported in Table 2. Note that all the considered pinpointing strategies lead to moderately increased iteration counts. The increase is most notable for (1 \triangleright), which effectively constrains a single point as the mesh is refined. On the other hand, strategies (3 \triangleright) and (3 \bullet), which always constrain all three components of the displacement in at least three points, yield the slowest growth rates. However, neither strategy yields convergent numerical solutions. In fact, the numerical error can often be seen to increase with resolution.

In the final example, a preconditioned CG method will be applied to solve the singular elasticity problem with data such that the compatibility conditions (2) are met.

Example 3. We consider a modified problem from Example 2, where f is not perturbed by rigid motions. As the data satisfy (2), the discrete linear system is solvable and amenable to a solution by the preconditioned CG method. To this end, the rigid motions are passed to the CG solver via the PETSc interface.[§] The mass or identity matrix is added to the singular system matrix in order to obtain a positive definite matrix in the construction of the preconditioner based on AMG. The first choice can be viewed as a simple mean to get an invertible system, whereas the motivation for the

[§]See *MatSetNullSpace* (<http://www.mcs.anl.gov/petsc/petsc-3.5/docs/manualpages/Mat/MatSetNullSpace.html>).

TABLE 3 Convergence of the preconditioned conjugate gradient method for the singular elasticity problem. Positive definite preconditioners using the mass and identity matrices to get a nonsingular system are considered. The maximum number of iterations is set to 150. The iterations are unbounded in both cases. Solutions due to a preconditioner using the identity matrix converge at a nearly optimal rate

Size	AMG(A + M)				AMG(A + I)			
	Kernel not removed		Kernel removed		Kernel not removed		Kernel removed	
	$\ u - u_h\ _1$	#	$\ u - u_h\ _1$	#	$\ u - u_h\ _1$	#	$\ u - u_h\ _1$	#
2,187	1.97E-02 (0.26)	17	5.08E-03 (0.99)	17	1.11E-02 (0.87)	21	5.08E-03 (0.99)	21
14,739	2.58E-02 (-0.39)	19	2.29E-03 (1.15)	19	2.87E-03 (1.95)	35	2.29E-03 (1.15)	35
107,811	2.80E-02 (-0.12)	34	1.06E-03 (1.11)	34	1.21E-03 (1.24)	81	1.06E-03 (1.11)	81
823,875	2.82E-02 (-0.01)	53	5.12E-04 (1.04)	54	6.32E-04 (0.94)	>150	5.12E-04 (1.04)	>150

Note. AMG = algebraic multigrid.

latter is the functional setting to be discussed later in Theorem 1. Moreover, for each preconditioner, two cases are considered where either the converged vector is postprocessed by removing from it the components of the null space or no postprocessing is applied. We note that, in this example, the iterations are started from a zero initial vector, and the relative tolerance of 10^{-10} is used as a convergence criterion. The number of iterations together with error and convergence rates based on the H^1 norm are reported in Table 3. We observe that the method with the mass matrix (cf. with the left pane of the table) yields convergent solutions only if postprocessing is applied. On the other hand, solutions with the preconditioner based on the identity matrix converge in the H^1 norm even if no postprocessing is used. The observation that the Krylov iterations/preconditioners respectively do and do not introduce rigid motions (recall that the initial guess and the right-hand side are orthogonal to the kernel) is related to the properties of the added matrices. A vector free of rigid motions remains orthogonal after applying to it the identity matrix. This property, in general, does not hold for the (not diagonal) mass matrix.

Examples 1–3 have illustrated some of the issues that might be encountered when solving the singular problem (1) with the FEM. In particular, the following questions may be posed: (a) What is the cause of the poor convergence properties of pinpointing? (b) What should be the order optimal preconditioner for CG? (c) What should be the order optimal preconditioner for the Lagrange multiplier formulation?

With questions (b) and (c) answered in detail in the remainder of the text, let us briefly comment on the first question. As will become apparent, the singular problem with a known kernel, such as (1), possesses all the information necessary to formulate a well-posed problem and a convergent numerical method. In this sense, coming up with a datum to be prescribed in the pinpointed nodes is theoretically redundant, but usually required for implementation. Further, as pointed out in the work of Bochev and Lehoucq,²⁶ there are stability issues with prescribing point values of H^1 functions for $d \geq 2$. However, we have not explored the settings of HypreAMG or other realizations of the preconditioner that could potentially improve the convergence properties of the method in Example 2. In this sense, the two-level preconditioner of Vanek et al.²⁸ is interesting as the proposed method results in bounded CG iterations even with the variationally problematic point boundary conditions.

3 | LAGRANGE MULTIPLIER FORMULATION

Let $Z \subset V = [H^1(\Omega)]^3$ denote the space of rigid motions of Ω . For compatible data, a unique solution u of (1) is required to be linearly independent of functions in Z . To this end, a Lagrange multiplier $p \in Z$ is introduced, which enforces the orthogonality of u with respect to Z . The constrained variational formulation of (1) seeks $u \in V, p \in Z$ such that[¶]

$$\begin{aligned} 2\mu(\epsilon(u), \epsilon(v)) + \lambda(\nabla \cdot u, \nabla \cdot v) - (p, v) &= (f, v) + (h, v)_{\partial\Omega} & \forall v \in V, \\ -(u, q) &= 0 & \forall q \in Z. \end{aligned} \quad (6)$$

[¶]Note that $(h, v)_{\partial\Omega}$ stands for the integral $\int_{\partial\Omega} h \cdot v \, ds$.

Equation (6) defines a saddle-point problem for $(u, p) \in W$, $W = V \times Z$ satisfying

$$\mathcal{A} \begin{pmatrix} u \\ p \end{pmatrix} = \begin{pmatrix} A & B \\ B' & \end{pmatrix} \begin{pmatrix} u \\ p \end{pmatrix} = \begin{pmatrix} l \\ 0 \end{pmatrix}, \tag{7}$$

where $l \in V'$ such that $\langle l, v \rangle = (f, v) + (h, v)_{\partial\Omega}$ and operators $A : V \rightarrow V'$, $B : Z \rightarrow V'$ are defined in terms of bilinear forms

$$a(u, v) = 2\mu(\epsilon(u), \epsilon(v)) + \lambda(\nabla \cdot u, \nabla \cdot v) \quad \text{and} \quad b(u, q) = (u, q) \tag{8}$$

as $\langle Au, v \rangle = a(u, v)$ and $\langle Bq, u \rangle = -b(u, q)$. We note that, in (7), the operator B' is the adjoint of B .

The existence and uniqueness of the solution to (7) follows from the Brezzi theory²⁹ (see also Chapter 3.4 in the work of Braess⁷). The proof shall utilize the inequalities given in Lemma 1.

Lemma 1. *Let $u \in V$ be arbitrary and $\omega(u)$ be the skew-symmetric part of the displacement gradient ∇u , that is, $\omega(u) = \frac{1}{2}((\nabla u) - (\nabla u)^\top)$. Then, we have*

$$\|\epsilon(u)\| \leq \|\nabla u\| \quad \text{and} \quad \|\omega(u)\| \leq \|\nabla u\|, \tag{9a}$$

$$\|\nabla \cdot u\| \leq \sqrt{3}\|\nabla u\|, \tag{9b}$$

$$\exists C = C(\Omega) \text{ such that } \|z\|_1 \leq C\|z\| \quad \forall z \in Z. \tag{9c}$$

Proof. Inequality (9a) follows from the orthogonal decomposition $\nabla u = \epsilon(u) + \omega(u)$. Inequality (9b) follows by direct calculations. To establish the final inequality, we first note that (9c) clearly holds for rigid motions that are translations with constant $C = 1$. To verify it for rigid rotations, we consider the representation $z = Sx$ for some arbitrary skew-symmetric matrix $S \in \mathbb{R}^{3 \times 3}$. Then, by definition, $\omega(Sx) = S$ so that $(\omega(z), \omega(z)) = |S|^2|\Omega|$, with $|S| = \sqrt{\text{tr}(S^\top S)}$ as the Frobenius norm. In turn, we have

$$\|z\|^2 = (Sx, Sx) = |S|^2(x, x) = \frac{(x, x)}{|\Omega|}(\omega(z), \omega(z)) = c(\Omega)\|\nabla z\|^2, \quad c(\Omega) = \frac{(x, x)}{|\Omega|} \tag{10}$$

as $\epsilon(z) = 0$. Therefore, (9c) holds for all rotations. We remark that the constant c in (10) is related to the moment of inertia of the body. Finally, the statement follows with a constant $C(\Omega) = \sqrt{1 + c(\Omega)}$ from the decomposition of any $z \in Z$ into translations and rotations. \square

Theorem 1. *Let f, h such that $l \in V'$. Then, there exists a unique solution $u \in V, p \in Z$ of (7).*

Proof. We proceed by establishing the Brezzi constants. First, the bilinear form a is shown to be bounded with respect to $\|\cdot\|_1$. Indeed, by the Cauchy–Schwarz inequality and inequalities (9a) and (9b), for any $u, v \in V$, we have

$$\begin{aligned} a(u, v) &= 2\mu(\epsilon(u), \epsilon(v)) + \lambda(\nabla \cdot u, \nabla \cdot v) \leq 2\mu\|\epsilon(u)\|\|\epsilon(v)\| + \lambda\|\nabla \cdot u\|\|\nabla \cdot v\| \\ &\leq (2\mu + 3\lambda)\|\nabla v\|\|\nabla u\| \leq \alpha^*\|u\|_1\|v\|_1 \end{aligned}$$

with $\alpha^* = 2\lambda + 3\mu$. The ellipticity of a on $Z^\perp = \{v \in V; (v, z) = 0 \forall z \in Z\} = \{v \in V; b(v, p) = 0 \forall p \in Z\}$ follows from Korn's inequality (5). Since $\lambda \geq 0$ by assumption, we have

$$a(u, u) = 2\mu\|\epsilon(u)\|^2 + \lambda\|\nabla \cdot u\|^2 \geq 2\mu\|\epsilon(u)\|^2 \geq \alpha_*\|u\|_1^2 \quad \forall u \in Z^\perp,$$

with $\alpha_* = 2\mu C$ and $C = C(\Omega)$ as the constant from (5). The boundedness of b with a constant $\beta^* = 1$ follows from the Cauchy–Schwarz inequality. Finally, using (9c), for arbitrary $p \in Z$, we have

$$\sup_{v \in V} \frac{b(v, p)}{\|v\|_1} \geq \frac{(p, p)}{\|p\|_1} \geq \frac{\|p\|^2}{C\|p\|} = \frac{1}{C}\|p\|$$

so that the inf-sup condition holds with $\beta_* = C^{-1}$, with C as the constant from (9c). \square

We remark that Theorem 1 implies that the operator $\mathcal{A} : W \rightarrow W'$ from (7) is an isomorphism. In particular, conditions (2) need not hold for there to exist a unique solution of (6). In order to find the solution of the well-posed (7) numerically, conditions from Theorem 1 must hold with discrete subspaces V_h and Z_h (see the work of Fortin³⁰ or Chapter 3.4 in the work of Braess⁷). Typically, satisfying the discrete inf-sup condition presents an issue and requires the choice of compatible finite element discretization of the involved spaces, for example, Taylor–Hood or MINI elements³¹ for the Stokes equations. For the conforming discretization $V_h \subset V, Z_h = Z$, the following result shows that the discrete inf-sup condition holds.

Theorem 2. Let $Z_h = Z$, $V_h \subset V$ and b be the bilinear form defined in (8). Then, there is a constant β_* independent of h such that $\inf_{p \in Z_h} \sup_{v \in V_h} \frac{b(v,p)}{\|v\|_1 \|p\|} \geq \beta_*$.

Proof. The proof mirrors the continuous inf-sup condition in Theorem 1. Let $p \in Z_h$ be given. Since $Z = Z_h \subset V_h$, by taking $v = p$, we get

$$\sup_{v \in V_h} \frac{b(v,p)}{\|v\|_1} \geq \frac{(p,p)}{\|p\|_1} \geq \frac{\|p\|^2}{C\|p\|} = \frac{1}{C}\|p\|,$$

where C is the constant from (9c). \square

Following Theorems 1 and 2 and operator preconditioning,^{24,32} the Riesz map $B_1 : W' \rightarrow W$ with respect to the inner product $(u, v)_1 + (p, q)$ with $(u, p), (v, q) \in W$

$$B_1 = \begin{pmatrix} H & \\ & I \end{pmatrix}^{-1}, \quad H : V \rightarrow V', \langle Hu, v \rangle = (u, v)_1 \quad \text{and} \quad I : Z \rightarrow Z', \langle Ip, q \rangle = (p, q) \quad (11)$$

defines a preconditioner for discretized (7) whose condition number is independent of h . This follows from the Brezzi constants in Theorems 1 and 2 being free of the discretization parameter.

Since applying the preconditioner (11) requires an inverse of the 6×6 mass matrix of the space rigid motions, it is advantageous to choose a basis of Z in which the matrix is well conditioned. With the choice of an L^2 orthonormal basis, the obtained mass matrix is an identity, and we shall therefore briefly discuss the construction of such a basis.

3.1 | Construction for orthonormal basis of rigid motions

Consider a unit cube $\Omega = \left[-\frac{1}{2}, \frac{1}{2}\right]^3$ centered at the origin. Denoting e_i , $i = 1, 2, 3$, as the canonical unit vectors, the set

$$Z_{\square} = \{e_1, e_2, e_3, x \times e_1, x \times e_2, x \times e_3\}$$

constitutes an orthonormal basis of the rigid motions of Ω with respect to the L^2 inner product. Clearly, the basis for an arbitrary body can be obtained from Z_{\square} by a Gram–Schmidt process. However, we shall advocate here a construction derived from physical considerations. The construction was originally presented by Kuchta et al.³³

Lemma 2. Let $c = |\Omega|^{-1}(x, 1)$ be the center of mass of Ω ; I_Ω be the tensor of inertia (see chapter 4 in the work of Gurtin³⁴) of Ω with respect to c , that is,

$$I_\Omega = \int_{\Omega} I(x-c)^T(x-c) + (x-c) \otimes (x-c) dx;$$

and (λ_i, v_i) , $i = 1, 2, 3$, be the eigenpairs of the tensor. Then, the set

$$Z_\Omega = \left\{ |\Omega|^{-\frac{1}{2}}v_1, |\Omega|^{-\frac{1}{2}}v_2, |\Omega|^{-\frac{1}{2}}v_3, \lambda_1^{-\frac{1}{2}}(x-c) \times v_1, \lambda_2^{-\frac{1}{2}}(x-c) \times v_2, \lambda_3^{-\frac{1}{2}}(x-c) \times v_3 \right\} \quad (12)$$

is the L^2 orthonormal basis of rigid motions of Ω .

Proof. Note that, by construction, I_Ω is a symmetric positive definite tensor. Thus, $\lambda_i > 0$, and there exists a complete set of eigenvectors $v_i^T v_j = \delta_{ij}$. We proceed to show that the Gram matrix of the proposed basis is an identity. First, $(v_i, v_j) = |\Omega|\delta_{ij}$ by orthonormality of the eigenvectors. Further, for $((x-c) \times v_i, v_j) = (v_i \times v_j, (x-c))$ and in the nontrivial case $i \neq j$, the product is zero since c is the center of mass. Finally, $((x-c) \times v_i, (x-c) \times v_j) = v_i^T I_\Omega v_j = \lambda_i \delta_{ij}$. \square

We remark that the rigid motions of the body are in the constructed basis given in terms of translations along and rotations around the principal axes of the tensor that describes its rotational kinetic energy.

Note also that the construction can be generalized to yield an orthonormal basis with respect to different inner products. In particular, let $Z_h = \text{span}\{z_k\}_{k=1}^6 \subset V_h$ be functions approximating some basis of Z . For $u, v \in V_h$, let $\mathbf{u} = \pi_h u$ and $\mathbf{v} = \pi_h v$ be coefficient vectors in the nodal basis of V_h . The l^2 orthonormal basis of Z_h can be created using Lemma 2 by replacing (u, v) with $\mathbf{u}^T \mathbf{v}$. The differences between the bases are shown in Figure 2, where the defining principal axes of the L^2 and l^2 orthonormal bases of rigid motions are drawn. If Ω is uniformly triangulated, the bases are practically identical. However, the l^2 basis changes in the presence of a nonuniform mesh refinement.

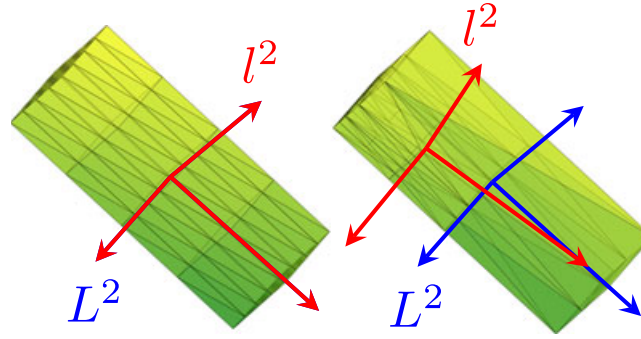


FIGURE 2 Computational domains considered in the numerical examples for linear elasticity are obtained by uniformly refining the parent mesh. (Left) Parent is close to uniformly triangulated. (Right) The parent mesh is refined near a single edge of the domain. The blue and red arrows indicate the principal axes of the tensor I_Ω (cf. Lemma 2), defined using the L^2 and l^2 inner products. Axes are drawn from the center of mass computed using the respected inner products. Only the L^2 basis is stable upon change of triangulation from uniform (left) to nonuniform (right)

Formulation of problem (6) with respect to an L^2 orthonormal basis $\{z_k\}_{k=1}^6$ of the space of rigid motions results in the mapping between Z and \mathbb{R}^6 , being an isometry. In turn, if the discretized problem is considered with space $V_h \times \mathbb{R}^6$ and its natural norm, the Brezzi constants will be those obtained in Theorem 2. On the other hand, for a nonorthonormal basis only, equivalence between the norms holds: There exists $C_1, C_2 > 0$ such that, for all $p \in Z$, we have

$$C_1|c| \leq \|p\| \leq C_2|c|, \quad p = \sum_{k=1}^6 c_k z_k,$$

and the constants C_1 and C_2 enter the estimates in the Brezzi theory. For an unfortunate choice of the basis, it is then possible that $C_1 = C_1(h)$ or $C_2 = C_2(h)$, leading to the mesh-dependent performance of a preconditioner using the l^2 norm for (the Lagrange multiplier space) \mathbb{R}^6 .

Returning to preconditioner (11), recall that the Brezzi constants α^*, α_* depend on the Lamé constants, and thus, \mathcal{B}_1 does not define a parameter robust preconditioner. To address the dependence on material parameters, we shall, at first, assume that μ and λ are comparable in magnitude. The case $\lambda \gg \mu$ is postponed until Section 6.

3.2 | Robust preconditioning of the singular problem

Parameter robust preconditioners for the Lagrange multiplier formulation of the singular elasticity problem (6) can be analyzed by the operator preconditioning framework of Mardal and Winther.²⁴ The preconditioners are constructed by considering (7) in parameter-dependent spaces (see, e.g., the work of Bergh and Löfström³⁵), which are equivalent with V as a set, but the topology of the spaces is given by different parameter-dependent norms. Two such norms, leading to two different preconditioners, are constructed next.

For $u \in V$, consider the orthogonal decomposition $u = u_Z + u_{Z^\perp}$, where $u_Z \in Z$ and $u_{Z^\perp} \in Z^\perp$. Bilinear forms $(\cdot, \cdot)_E$ and $(\cdot, \cdot)_M$ over V are defined in terms of A from (7) and operators $Y : V \rightarrow V'$ and $M : V \rightarrow V'$ as

$$\begin{aligned} \langle Yu, v \rangle &= (u_Z, v_Z), & (u, v)_E &= \langle Au, v \rangle + \langle Yu, v \rangle, \\ \langle Mu, v \rangle &= (u, v), & (u, v)_M &= \langle Au, v \rangle + \langle Mu, v \rangle. \end{aligned} \tag{13}$$

The forms (13) define functionals $\|\cdot\|_E$ and $\|\cdot\|_M$ over V such that

$$\|u\|_E = \sqrt{(u, u)_E} \quad \text{and} \quad \|u\|_M = \sqrt{(u, u)_M}. \tag{14}$$

Lemma 3. *Let $\|\cdot\|_E$ and $\|\cdot\|_M$ be the functionals (14). Then, $\|\cdot\|_E$ and $\|\cdot\|_M$ define norms on V , which are equivalent with the H^1 norm.*

Proof. From the orthogonal decomposition of $u \in V$, it follows that $\|u\|_M^2 = \|u\|_E^2 + \|u_{Z^\perp}\|^2$. Together with Lemma 1, we thus establish

$$\|u\|_E^2 \leq \|u\|_M^2 \leq (2\mu + 3\lambda + 1)\|u\|_1^2 \quad \forall u \in V.$$

To complete the equivalence, let $C = C(\Omega)$ be the constant from Korn's inequality (4). Then, for all $u \in V$, we have

$$\|u\|_M^2 \geq 2\mu\|\epsilon(u)\|^2 + \|u\|^2 \geq c\|u\|_1^2,$$

with $c = C$ for $2\mu > 1$ and $c = 2\mu C$ otherwise. Finally, for the equivalence of the E -norm, Korn's inequality on Z^\perp (see (5) and Theorem 1) yields

$$\|u\|_E^2 = 2\mu\|\epsilon(u)\|^2 + \lambda\|\nabla \cdot u\|^2 \geq 2\mu C\|u\|_1^2 \quad \forall u \in Z^\perp$$

with $C = C(\Omega)$, whereas using (9c) in Lemma 1 gives

$$\|u\|_E = \|u\| \geq C_1(\Omega)\|u\|_1$$

for any $u \in Z$. Thus, E and H^1 norms are equivalent on Z^\perp and Z , respectively. The proof is completed by observing that u_Z and u_{Z^\perp} satisfy $(u_Z, u_{Z^\perp})_E = 0$ so that

$$\|u\|_E^2 = 2\mu\|\epsilon(u_{Z^\perp})\|^2 + \lambda\|\nabla \cdot u_{Z^\perp}\|^2 + \|u_Z\|^2 \geq 2\mu C\|u_{Z^\perp}\|_1^2 + C_1\|u_Z\|_1^2 \geq c(\|u_{Z^\perp}\|_1^2 + \|u_Z\|_1^2),$$

$c = \min(2\mu C, C_1)$, whereas for the H^1 inner product, $\|u\|_1^2 \leq 2(\|u_{Z^\perp}\|_1^2 + \|u_Z\|_1^2)$ holds. Thus, $\|u\|_E^2 \geq \frac{c}{2}\|u\|_1^2$ for all $u \in V$. \square

Using equivalent norms of V from Lemma 3, we readily establish equivalent norms for the product space $W = V \times Z$, that is,

$$\|w\|_E = \|(u, p)\|_E = \sqrt{\|u\|_E^2 + \|p\|^2} \quad \text{and} \quad \|w\|_M = \|(u, p)\|_M = \sqrt{\|u\|_M^2 + \|p\|^2}, \quad (15)$$

and consider as preconditioners for (7) the operators $\mathcal{B}_E : W' \rightarrow W$ and $\mathcal{B}_M : W' \rightarrow W$, that is,

$$\mathcal{B}_E = \begin{pmatrix} A + Y & \\ & I \end{pmatrix}^{-1} \quad \text{and} \quad \mathcal{B}_M = \begin{pmatrix} A + M & \\ & I \end{pmatrix}^{-1}. \quad (16)$$

Note that the mappings (16) are the Riesz maps with respect to the inner products that induce norms (15). We proceed with the analysis of the properties of \mathcal{B}_E .

Theorem 3. *Let $\mathcal{A} : W \rightarrow W'$ be the operator and the space from (7) and W_E be the space W considered with the $\|\cdot\|_E$ norm (15). Then, $\mathcal{A} : W_E \rightarrow W'_E$ is an isomorphism. Moreover, the Riesz map $\mathcal{B}_E : W'_E \rightarrow W_E$ in (16) defines the canonical preconditioner for (7).*

Proof. We shall show that the first assertion holds by establishing the Brezzi constants. Recall the definition of the bilinear form a given in (8). Then, by the Cauchy–Schwarz inequality and (9a) in Lemma 1, the inequality $a(u, v) \leq \sqrt{a(u, u)}\sqrt{a(v, v)}$ holds for any $u, v \in V$. In turn, for all $u, v \in V$, we have

$$a(u, v) \leq \sqrt{a(u, u)}\sqrt{a(v, v)} \leq \sqrt{a(u, u) + (u_Z, u_Z)}\sqrt{a(v, v) + (v_Z, v_Z)} = \|u\|_E\|v\|_E,$$

and a is bounded with respect to the E norm with a constant $\alpha^* = 1$. Further, $u_Z = 0$ for $u \in Z^\perp$. Hence, $a(u, u) = a(u, u) + (u_Z, u_Z) = \|u\|_E^2$ for all $u \in Z^\perp$, and the form is E elliptic on Z^\perp with constant $\alpha^* = 1$. To compute the boundedness constant of the form b , the orthogonal decomposition $u = u_Z + u_{Z^\perp}$ is used so that, for all $u \in V, q \in Z$, we have

$$b(u, q) = (u_Z + u_{Z^\perp}, q) = (u_Z, q) \leq \|u_Z\|\|q\| = \sqrt{a(u, u) + \|u_Z\|^2}\|q\| = \|u\|_E\|q\|,$$

and we have $\beta^* = 1$. Finally, taking any $q \in Z$ and setting $u = q$ in

$$\sup_{u \in V} \frac{b(u, q)}{\|u\|_E} \geq \frac{(q, q)}{\sqrt{a(q, q) + (q_Z, q_Z)}} = \frac{\|q\|^2}{\sqrt{0 + \|q\|^2}} \geq \|q\|,$$

the inf-sup condition holds with $\beta_* = 1$. As all the constants are independent of material parameters, the second assertion follows from the first one by operator preconditioning (see chapter 5 in the work of Mardal and Winther²⁴). \square

Using Theorem 3, it is readily established that the condition number of the composed operator $\mathcal{B}_E \mathcal{A} : W \mapsto W$ is equal to 1. We further note that discretizing operator \mathcal{B}_E leads to discrete null space preconditioners as in chapter 6 in the work of Benzi et al.³⁶

While the spectral properties of \mathcal{B}_E are appealing, the preconditioner is impractical. Consider \mathbf{B}_E as a matrix representation of the Galerkin approximation of \mathcal{B}_E in $W_h \subset W$. Then, $\mathbf{B}_E = \text{diag}(\mathbf{A} + \mathbf{Y}\mathbf{Y}^\top, \mathbf{I})^{-1}$, where $\mathbf{Y} = \mathbb{R}^{n \times 6}$,

$\mathbf{y}_k = \text{col}_k \mathbf{Y} = \pi_h z_k$, and $z_k \in V_h$ is the function from the L^2 orthogonal basis of the space of rigid motions. Due to the second (nonlocal) term, the matrix $\mathbf{A} + \mathbf{Y}\mathbf{Y}^\top$ is dense. Further, as shall be discussed in Section 4, inverting the operator requires computing (the action of) the pseudoinverse of the singular matrix \mathbf{A} . The mapping \mathcal{B}_M , on the other hand, leads to a more practical preconditioner.

Theorem 4. *Let $\mathcal{A} : W \rightarrow W'$ be the operator and space defined in (7) and W_M be defined analogically to Theorem 3. Then, $\mathcal{A} : W_M \rightarrow W'_M$ is an isomorphism. Moreover, the Riesz map $\mathcal{B}_M : W'_M \rightarrow W_M$ in (16) defines a parameter robust preconditioner for (7).*

Proof. As in the proof of Theorem 3, we establish that $a(u, v) \leq \|u\|_M \|v\|_E$ for all $u, v \in V$ and $b(v, p) \leq \|v\| \|p\| \leq \|v\|_M \|p\|$ for all $v \in V, p \in Z$. Setting $v = p \in Z$ then yields $\inf_{p \in Z} \sup_{v \in V} \frac{b(v, p)}{\|v\|_M \|p\|} \geq 1$. For M ellipticity of a on Z^\perp , assume the existence of $C = C(\Omega)$ such that $\|u\|^2 \leq C \|\epsilon(u)\|^2$ for all $u \in Z^\perp$. Then, on Z^\perp , we have

$$\|u\|^2 \leq C \|\epsilon(u)\|^2 \leq C \mu \|\epsilon(u)\|^2 \leq C (2\mu \|\epsilon(u)\|^2 + \lambda \|\nabla \cdot u\|^2) = C \|u\|_E^2$$

and

$$\|u\|_M^2 = \|u\|_E^2 + \|u\|^2 \leq (C + 1) \|u\|_E^2$$

so that $a(u, u) = \|u\|_E^2 \geq (1 + C)^{-1} \|u\|_M^2$. Finally, we comment on the assumption of the existence of constant C . Assume the contrary. Then, there is $u \in Z^\perp$ such that $\|\epsilon(u)\| = 1, \|w(u)\| = 0$ and the $\|u\|$ unbounded. However, such u violates Korn's inequality (5). \square

We remark that Theorem 4 required an additional assumption $2\mu \geq 1$. The assumption is not restrictive as it can be always achieved by scaling the equations such that the inequality is satisfied. Note also that with the orthonormal basis of rigid motions, the discrete preconditioner based on \mathcal{B}_M is such that $\mathbf{B}_M^{-1} = \text{diag}(\mathbf{A} + \mathbf{M}, \mathbf{I})$, with \mathbf{M} as the mass matrix. The system to be assembled is therefore sparse.

Following Theorem 4, the condition number of the preconditioned operator $\mathcal{B}_M \mathcal{A} : W \rightarrow W$ depends solely on constant C from Korn's inequality (5). An approximation for the constant is provided by the smallest positive eigenvalue λ_{\min}^+ of the problem

$$\begin{pmatrix} \mathbf{A} & \mathbf{B} \\ \mathbf{B}^\top & \mathbf{0} \end{pmatrix} \begin{pmatrix} \mathbf{u} \\ \mathbf{p} \end{pmatrix} = \lambda \begin{pmatrix} \mathbf{A} + \mathbf{M} & \mathbf{0} \\ \mathbf{0} & \mathbf{I} \end{pmatrix} \begin{pmatrix} \mathbf{u} \\ \mathbf{p} \end{pmatrix}.$$

In Table A1 of the Appendix, the constant has been computed for two different domains: a cube from Example 2 and a hollow cylinder. In both cases, $C \approx 1$ can be observed.

In order to demonstrate h robust properties of \mathcal{B}_M , the problem from Example 2 is considered with the basis from Section 3.1 and discretized on $V_h \subset V$. The resulting preconditioned linear system is solved by the minimal residual (MinRes) method³⁷ as implemented in *cbc.block*, the FEniCS library for block matrices³⁸ using as the preconditioner

$$\mathbf{B}_M = \begin{pmatrix} \text{AMG}(\mathbf{A} + \mathbf{M}) & \mathbf{0} \\ \mathbf{0} & \mathbf{I} \end{pmatrix}.$$

More specifically, the preconditioner uses a single AMG V cycle with one pre- and postsmoothing by a symmetric successive over-relaxation smoother. The rigid motions were not passed to the routine on initialization. The saddle-point system was assembled and inverted[#] using *cbc.block*. The results of the experiment are presented in Table 5. Clearly, the number of iterations required for convergence is independent of the discretization. Moreover, the method yields numerical solutions that converge in the H^1 norm at the optimal rate^{||} on both the uniform and nonuniform meshes (cf. Figure 2).

A drawback of the Lagrange multiplier formulation is the cost of solving the resulting indefinite linear system. Following, for example, chapter 7.2 in the work of Greenbaum,³⁹ let the condition number of a Hermitian matrix \mathbf{A} be $\kappa(\mathbf{A}) = \lambda_{\max}(\mathbf{A})/\lambda_{\min}(\mathbf{A})$, where $\lambda_{\max}(\mathbf{A})$ and $\lambda_{\min}(\mathbf{A})$ are the largest and smallest (in magnitude) eigenvalues of the matrix, respectively. For \mathbf{A} as Hermitian indefinite and under simplifying assumptions on the spectrum, chapter 3.2 in the work of Liesen and Tichý⁴⁰ gives the following bound on the relative error in residual r_n at step n of the MinRes method, that is,

$$\frac{|r_n|}{|r_0|} \leq 2 \left(\frac{\kappa(\mathbf{A}) - 1}{\kappa(\mathbf{A}) + 1} \right)^{n/2}.$$

[#] The implementation of the solver as well as the two algorithms discussed in Sections 5 and 6 can be found online at <https://github.com/MiroK/fenics-rigid-motions>.

^{||} We recall that V_h is constructed from continuous linear Lagrange elements.

The result should be contrasted with a similar one for the error e_n at the n th step of the CG method on symmetric positive definite matrix \mathbf{A} (see, e.g., Theorem 38.5 in the work of Trefethen and Bau⁴¹), that is,

$$\frac{e_n^\top \mathbf{A} e_n}{e_0^\top \mathbf{A} e_0} \leq 2 \left(\frac{\sqrt{\kappa(\mathbf{A})} - 1}{\sqrt{\kappa(\mathbf{A})} + 1} \right)^n.$$

While the above estimates are known to give the worst case behavior of the two methods, the faster rate of convergence of the CG motivates investigating formulations of (1) to which the CG method can be applied.

4 | CG METHOD FOR DISCRETE SINGULAR PROBLEMS

We consider a variational formulation of (1): Find $u \in V = [H^1(\Omega)]^3$ such that

$$2\mu(\varepsilon(u), \varepsilon(v)) + \lambda(\nabla \cdot u, \nabla \cdot v) = (f, v) + (h, v)_{\partial\Omega} \quad \forall v \in V. \quad (17)$$

Denoting $a : V \times V \rightarrow \mathbb{R}$, $l : V' \rightarrow \mathbb{R}$ as the bilinear and linear forms defined by (17), we note that the problem is not well-posed in V . Indeed, the compatibility conditions (2) restrict the functionals for which the solution can be found to be $l \in Z^0 = \{f \in V'; \langle f, z \rangle = 0 \forall z \in Z\}$. Moreover, only the part of u in Z^\perp is uniquely determined by (17). More precisely, we have the following result.

Theorem 5. *Let $l \in Z^0$. Then, there exists a unique solution of the problem:*

$$\text{Find } u \in Z^\perp \text{ such that for any } v \in Z^\perp, \text{ it holds that } a(u, v) = \langle l, v \rangle. \quad (18)$$

Proof. The complete proof can be found as Theorem 11.2.30 in the work of Brenner and Scott.⁴² Note that the boundedness and ellipticity of a on Z^\perp with $\|\cdot\|_1$ are proven as part of Theorem 1. \square

We remark that if (2) holds, then $u \in Z^\perp$ solves (18) if and only if $(u, 0)$ solves the Lagrange multiplier problem (7). Further, the well-posed variational problem (18) is not suitable for discretization by the FEM as the approximation leads to a dense linear system. A sparse discrete problem to which the CG method shall be applied is therefore derived from (17).

Recall $\dim Z = 6$, $n = \dim V_h$, and let $V_h = \text{span}\{\phi_i\}_{i=1}^n$. Discretizing the variational problem (17) leads to a linear system

$$\mathbf{A} \mathbf{u} = \mathbf{b}, \quad (19)$$

where $\mathbf{A} \in \mathbb{R}^{n \times n}$ such that $A_{ij} = a(\phi_j, \phi_i)$ and vector $\mathbf{b} \in \mathbb{R}^n$, $b_i = \langle l, \phi_i \rangle$. Note that we shall consider (19) for a general right-hand side, that is, not necessarily a discretization of $l \in Z^0$. We proceed by reviewing the properties of the discrete system.

Due to the symmetry and ellipticity of the bilinear form a on Z^\perp , there exists, respectively, six vectors \mathbf{z}_k and $n - 6$ eigenpairs (γ_i, \mathbf{u}_i) , $\gamma_i > 0$ such that $\mathbf{A} \mathbf{z}_k = 0$, $\mathbf{z}_k^\top \mathbf{u}_i = 0$, $\mathbf{A} \mathbf{u}_i = \gamma_i \mathbf{u}_i$, and $\mathbf{u}_i^\top \mathbf{u}_j = \delta_{ij}$. From the decomposition of \mathbf{A} , it follows that system (19) is solvable if and only if $\mathbf{z}_k^\top \mathbf{b} = 0$ for any k , and the unique solution of the system is $\mathbf{u} \in \text{span}\{\mathbf{u}_i\}_{i=1}^{n-6}$. We note that the last statement is the Fredholm alternative for (19). As a further consequence of the decomposition, it is readily verified that given compatible vector \mathbf{b} , the solution of (19) is $\mathbf{u} = \mathbf{B}_A \mathbf{b}$ with \mathbf{B}_A such that $\mathbf{B}_A \mathbf{y} = \sum_i \gamma_i^{-1} (\mathbf{u}_i^\top \mathbf{y}) \mathbf{u}_i$. The matrix \mathbf{B}_A is the pseudoinverse⁴³ or natural inverse (see chapter 3 in the work of Lanczos⁴⁴) of \mathbf{A} .

We note that any vector from \mathbb{R}^n can be orthogonalized with respect to the kernel of \mathbf{A} by a projector $\mathbf{P}_Z = \mathbf{I} - \mathbf{Z} \mathbf{Z}^\top$, where $\mathbf{Z} \in \mathbb{R}^{n \times 6}$ is the matrix consisting of l^2 orthonormal basis vectors of the kernel.

With \mathbf{b} such that $\mathbf{Z}^\top \mathbf{b} = 0$, the solution \mathbf{u} of linear system (19) can be computed by the CG method.⁴⁵ Let \mathbf{u}^0 be the starting vector for the iterations. Then, assuming exact arithmetic and no preconditioner, the method preserves the component of \mathbf{u}^0 in \mathbf{Z} , that is, $\mathbf{Z}^\top \mathbf{u}^0 = \mathbf{Z}^\top \mathbf{u}$. In particular, $\mathbf{Z}^\top \mathbf{u}^0 = 0$ is required to obtain a solution orthogonal to the kernel. On the other hand, let \mathbf{B} be the CG preconditioner. Then, the iterations introduce components of the kernel to the solution even if $\mathbf{Z}^\top \mathbf{u}^0 = 0$, unless the range of \mathbf{B} is orthogonal to \mathbf{Z} .

4.1 | Preconditioned CG for the singular elasticity problem

A suitable preconditioner for (19) is obtained by a composition with the \mathbf{P}_Z projector, and we shall consider $\mathbf{B}_M = \mathbf{P}_Z (\mathbf{A} + \mathbf{M})^{-1}$, where \mathbf{M} is the mass matrix. That the preconditioner leads to a bounded iteration count (and converging

TABLE 4 Preconditioned conjugate gradient iterations on (19) obtained by the discretization of (17) with problem parameters as in Example 2 and two preconditioners. Both systems are solved with relative tolerance of 10^{-10} . A uniform mesh is used

Size	$\mathbf{P}_Z\text{AMG}(\mathbf{A} + \mathbf{M})$			$\text{AMG}(\mathbf{A} \mathbf{Z})$		
	$\ u - u_h\ _1$	#	Time [s]	$\ u - u_h\ _1$	#	Time [s]
14,739	1.14E-02 (1.09)	22	0.491	1.14E-02 (1.09)	21	0.537
107,811	5.49E-03 (1.06)	23	10.17	5.49E-03 (1.06)	23	10.96
823,875	2.71E-03 (1.02)	24	103.5	2.71E-03 (1.02)	25	86.51
6,440,067	1.35E-03 (1.00)	26	1,580	1.35E-03 (1.00)	26	911.9

Note. AMG = algebraic multigrid.

TABLE 5 Convergence properties of (top) the Lagrange multiplier formulation (7) and (bottom) the singular formulation (17) utilizing the l^2 orthogonal basis of the null space to invert system (19). Only the multiplier formulation yields solutions converging on uniform and nonuniform meshes. Relative tolerances of 10^{-11} and 10^{-10} are used for the minimal residual and conjugate gradient methods, respectively

Size	Uniform			Size	Refined		
	$\ u - u_h\ _1$	#	$\max_Z (u_h, z) $		$\ u - u_h\ _1$	#	$\max_Z (u_h, z) $
14,745	1.03E-02 (1.14)	44	3.54E-07	13,080	3.11E-02 (0.99)	50	1.68E-07
107,817	4.84E-03 (1.09)	45	2.77E-06	98,052	1.41E-02 (1.14)	53	6.73E-08
823,881	2.36E-03 (1.03)	45	1.38E-06	759,546	6.53E-03 (1.11)	54	8.11E-07
6,440,073	1.18E-03 (1.00)	44	1.75E-05	5,978,835	3.20E-03 (1.03)	55	2.94E-06
14,739	1.14E-02 (1.09)	21	1.30E-03	13,074	5.51E-02 (0.45)	26	6.06E-03
107,811	5.49E-03 (1.06)	23	6.66E-04	98,046	5.05E-02 (0.12)	27	6.32E-03
823,875	2.71E-03 (1.02)	25	3.36E-04	759,540	5.00E-02 (0.02)	29	6.43E-03
6,440,067	1.35E-03 (1.00)	26	1.69E-04	5,978,829	4.98E-02 (0.01)	31	6.49E-03

numerical solutions) is demonstrated in Table 4 (cf. left pane). The preconditioner is also compared with a different preconditioner based on the approximation of the pseudoinverse \mathbf{B}_A . The approximation can be constructed by passing a kernel of the operator to the CG routine, in the form of the l^2 orthonormal basis vectors (see *MatSetNullSpace* in PETSc²⁰). Note that the preconditioners perform similarly in terms of the iteration count; however, for large systems, the pseudoinverse appears to be a faster method.

We remark that in terms of operator preconditioning, the preconditioner based on the pseudoinverse can be interpreted as a Riesz map $Z^0 \rightarrow Z^\perp$ defined with respect to the inner product induced by the bilinear form a . Recall that a is symmetric and elliptic on Z^\perp . On the other hand, \mathbf{B}_M approximates a mapping $Z^0 \rightarrow V \rightarrow Z^\perp$.

Having established preconditioners for the indefinite system stemming from the Lagrange multiplier formulation (7) and the positive semidefinite problem stemming from (17), we shall finally discuss the approximation properties of the computed solutions. To this end, the problem from Example 2 is considered, where f is perturbed by rigid motions. Note that while with the new functional l , problem (7) is well-posed, in (19), a compatible right-hand side \mathbf{b} will be obtained by projector \mathbf{P}_Z .

The results of the experiment are listed in Table 5. The Lagrange multiplier method converges at an optimal rate on both uniformly and nonuniformly discretized meshes (cf. Figure 2). On the other hand, solutions to (19) converge to the true solution *only* on the uniform mesh, whereas there is no convergence with nonuniform discretization. Note that this is not signaled by the growth of the iterations: For both methods, the iteration counts are bounded. Note also that MinRes takes about twice as many iterations as CG.

From the experiment, we conclude that the CG method for (19), as applied so far, generally does not yield converging numerical solutions of (17). It is next shown that the issue is due to projector $\mathbf{P}_Z = \mathbf{I} - \mathbf{Z}\mathbf{Z}^\top$, which the method uses and which is derived from the discrete problem. In particular, we show that \mathbf{P}_Z is not a correct discretization of a projector used in the continuous problem (18) (and (7)). Following the continuous problem, a modification to CG is proposed, which leads to a converging method.

4.2 | CG method with Z^0, Z^\perp projectors

Consider the variational problem (18), which was proven well-posed in Theorem 5 under the assumptions $l \in Z^0 \subset V'$ and $u \in Z^\perp \subset V$. In this respect, there are two subspaces associated with (18), and we shall define two projectors $P : V \rightarrow Z^\perp$ and $P' : V' \rightarrow Z^0$ such that, for $u \in V, f \in V'$, we have

$$\begin{aligned} (Pu, v) &= (u_{Z^\perp}, v) \quad \forall v \in V, \\ \langle P'f, u \rangle &= \langle f, u - u_Z \rangle. \end{aligned} \quad (20)$$

Similar projectors were discussed in the work of Bochev and Lehoucq²⁶ for the singular Poisson problem. We note that $\langle f, Pu \rangle = \langle P'f, u \rangle$, and thus, P' is the adjoint of P .

Lemma 4. *Let $l \in V'$ and P, P' be the projectors (20). Then, $(u, p) \in V \times Z$ solves (7) with the right-hand side $(v, q) \mapsto \langle l, v \rangle + \langle 0, q \rangle$ if and only if $u \in Z^\perp$ and u solves (18) with the right-hand side $P'l$.*

Proof. It suffices to establish the relation between the right-hand sides. Testing (7) with $(z, 0)$, $z \in Z$ yields that $\langle p, z \rangle = \langle l, z \rangle$. In turn, for any $v \in V$, we have

$$\langle l, v \rangle - \langle p, v \rangle = \langle l, v \rangle - \langle p, v_Z + v_{Z^\perp} \rangle = \langle l, v \rangle - \langle l, v_Z \rangle = \langle l, v - v_Z \rangle = \langle l, Pv \rangle,$$

and the new right-hand side of (7) is therefore $(v, q) \mapsto \langle P'l, v \rangle + \langle 0, q \rangle$. \square

To derive a matrix representation of the projectors with respect to nodal basis $V_h = \text{span}\{\phi_i\}_{i=1}^n$, the mappings $\pi_h : V_h \rightarrow \mathbb{R}^n$ (the nodal interpolant) and $\mu_h : V'_h \rightarrow \mathbb{R}^n$ from (3) are used. We recall that $(u, v) = \mathbf{v}^\top \mathbf{M} \mathbf{u}$ for $\mathbf{u} = \pi_h u$, $\mathbf{v} = \pi_h v$ and $\mathbf{M}, M_{ij} = (\phi_j, \phi_i)$ as the mass matrix, whereas $\langle f, v \rangle = \mathbf{f}^\top \mathbf{v}$ with $\mathbf{f} = \mu_h f$. Finally, matrix $\mathbf{Y} = \mathbb{R}^{n \times 6}$ is such that $\mathbf{y}_k = \text{col}_k \mathbf{Y} = \pi_h z_k$, where $z_k \in V_h$ belongs to the L^2 orthogonal basis of the space of rigid motions. Then, we have

$$\begin{aligned} \mathbf{v}^\top \mathbf{M} \mathbf{P} \mathbf{u} &= (Pu, v) = (u, v) - \sum_{k=1}^6 (u, z_k)(v, z_k) = \mathbf{v}^\top \mathbf{M} (\mathbf{I} - \mathbf{Y} \mathbf{Y}^\top \mathbf{M}) \mathbf{u}, \\ \mathbf{f}^\top \mathbf{P}'^\top \mathbf{v} &= \langle f, Pv \rangle = \langle f, v \rangle - \sum_{k=1}^6 \langle f, z_k \rangle (v, z_k) = \mathbf{f}^\top (\mathbf{I} - \mathbf{Y} \mathbf{Y}^\top \mathbf{M}) \mathbf{v}, \end{aligned} \quad (21)$$

and $\mathbf{P} = (\mathbf{I} - \mathbf{Y} \mathbf{Y}^\top \mathbf{M})$ is the representation of P , whereas P' is represented by \mathbf{P}^\top . We remark that, in addition to \mathbf{Y} , the rigid motions $Z_h = \text{span}\{z_k\}_{k=1}^6$ can be represented in \mathbb{R}^n by an additional matrix $\mathbf{W} = \mathbf{M} \mathbf{Y}$, which is μ_h applied to functionals $v \mapsto (z_k, v)$. Following the work of Mardal and Winther,²⁴ matrices \mathbf{Y} and \mathbf{W} are respectively termed the primal and dual representations of Z_h . Observe that in (21), matrix \mathbf{P} uses the primal representation for \mathbf{u} , whereas the vector is expanded in the dual representation by \mathbf{P}' . Moreover, the L^2 orthogonality of Z_h yields $\mathbf{y}_i^\top \mathbf{w}_j = \delta_{ij}$. Finally, note that the projectors \mathbf{P}^\top and \mathbf{P} are implicitly present in the linear system, which is the discretization of the multiplier problem (7) with the orthogonal basis of rigid motions, that is,

$$\begin{pmatrix} \mathbf{A} & \mathbf{W} \\ \mathbf{W}^\top & \mathbf{P} \end{pmatrix} \begin{pmatrix} \mathbf{u} \\ \mathbf{p} \end{pmatrix} = \begin{pmatrix} \mathbf{b} \\ \mathbf{0} \end{pmatrix}. \quad (22)$$

Indeed, $\mathbf{p} = \mathbf{Y}^\top \mathbf{b}$ from premultiplying the first equation by \mathbf{Y}^\top . Upon substitution, the equation reads $\mathbf{A} \mathbf{u} = \mathbf{b} - \mathbf{W} \mathbf{Y}^\top \mathbf{b} = \mathbf{P}^\top \mathbf{b}$. Further, the solution is such that $\mathbf{P} \mathbf{u} = \mathbf{0}$.

The situation where the continuous problems (7) and (18) and the discrete problem (22) use different projectors for the left- and right-hand sides contrasts with (19), which utilizes \mathbf{P}_Z to obtain a consistent right-hand side, and the solution is such that $\mathbf{P}_Z \mathbf{u} = \mathbf{0}$ as well. This observation together with the lack of convergence of the CG method (cf. Table 5) motivate that the CG method on (19) is used with the following two modifications: (a) the iterations are started from vector $\mathbf{P}^\top \mathbf{b}$ and (b) \mathbf{P} is applied to the final solution.

The effect of the proposed modifications is shown in Table 6. The problem from Example 2 is considered on a nonuniform mesh, and the CG on (19) is applied with different combinations of projectors used to obtain the right-hand side from incompatible vector \mathbf{b} and to orthogonalize the converged solution. We observe that only the case $(\mathbf{P}^\top, \mathbf{P})^{**}$ yields optimal convergence. With $(\mathbf{P}_Z, \mathbf{P})$, the rate is slightly smaller than 1. In the remaining two cases, the solutions do not converge, suggesting that, for convergence, \mathbf{P} must be applied to the solution.

**Elements of the tuple denote the projector for the right-hand side and the left-hand side, respectively.

TABLE 6 Convergence of the conjugate gradient solutions for (19) with different combinations of the right-hand (horizontal) side and left-hand side (vertical) projectors. The problem from Example 2 is considered. Preprocessing the right-hand side and postprocessing the solution by projectors (\mathbf{P}^\top , \mathbf{P}) yield solutions converging at an optimal rate

	Size	\mathbf{P}_Z			\mathbf{P}^\top		
		$\ \mathbf{u} - \mathbf{u}_h\ _1$	#	$\max_Z (\mathbf{u}_h, \mathbf{z}) $	$\ \mathbf{u} - \mathbf{u}_h\ _1$	#	$\max_Z (\mathbf{u}_h, \mathbf{z}) $
\mathbf{P}_Z	13,074	5.51E-02 (0.45)	26	6.06E-03	5.53E-02 (0.44)	27	6.05E-03
	98,046	5.05E-02 (0.12)	27	6.32E-03	5.11E-02 (0.12)	28	6.31E-03
	759,540	5.00E-02 (0.02)	29	6.43E-03	5.06E-02 (0.01)	29	6.42E-03
	5,978,829	4.98E-02 (0.01)	31	6.49E-03	5.05E-02 (0.00)	31	6.48E-03
\mathbf{P}	13,074	3.13E-02 (0.98)	27	6.84E-16	3.11E-02 (0.99)	25	6.15E-16
	98,046	1.45E-02 (1.11)	28	2.94E-14	1.41E-02 (1.14)	27	2.92E-14
	759,540	6.92E-03 (1.07)	29	6.39E-14	6.53E-03 (1.11)	29	6.40E-14
	5,978,829	3.63E-03 (0.93)	31	2.89E-13	3.20E-03 (1.03)	31	2.86E-13

The results shown in Table 6 are satisfactory in a sense that preprocessing the right-hand side with \mathbf{P}^\top and postprocessing the solution with \mathbf{P} improved the convergence properties of the CG method for (19). However, the modifications alter the original discrete problem, and thus, the properties of the new problem should be discussed. We note that in the discussion, \mathbf{Z} and \mathbf{Y} are respectively the \mathbf{I} and \mathbf{M} orthogonal bases of the null space of \mathbf{A} . Further, the transformation matrix between the bases is $c \in \mathbb{R}^{6 \times 6}$ such that $\mathbf{Z} = \mathbf{Y}c$, and we have $\mathbf{Y}^\top \mathbf{M} \mathbf{Z} = c$.

First, the admissibility of the modified right-hand side $\mathbf{P}^\top \mathbf{b}$ is considered. Using the transformation matrix, it holds that $\mathbf{Z}^\top \mathbf{P}^\top \mathbf{b} = 0$, and thus, $\mathbf{P}^\top \mathbf{b}$ is compatible, and the solution can be obtained by a pseudoinverse (or equivalently by CG). The computed solution of the new linear system then satisfies $\mathbf{Z}^\top \mathbf{u} = 0$. However, the continuous problem requires orthogonality $\mathbf{Y}^\top \mathbf{M} \mathbf{u} = Ch$. As the two conditions are related through $|\mathbf{Y}^\top \mathbf{M} \mathbf{u}|^2 = \mathbf{u}^\top \mathbf{M} \mathbf{Z} (c^\top c)^{-1} \mathbf{Z}^\top \mathbf{M} \mathbf{u} = \mathbf{u}^\top \mathbf{M} \mathbf{Z} (\mathbf{Z}^\top \mathbf{M} \mathbf{Z})^{-1} \mathbf{Z}^\top \mathbf{M} \mathbf{u}$ and $\mathbf{Z}^\top \mathbf{Z} = \mathbf{I}$, the orthogonality in the L^2 inner product depends on the similarity of the mass matrix with identity. This is essentially a condition on the mesh, and $|\mathbf{Y}^\top \mathbf{M} \mathbf{Z}| \geq C$ is possible (as observed in Table 6).

To enforce the orthogonality constraint $\mathbf{Y}^\top \mathbf{M} \mathbf{u} = 0$ without postprocessing, we shall finally consider the linear system $\mathbf{A} \mathbf{u} = \mathbf{P}^\top \mathbf{b}$ and require $\mathbf{P} \mathbf{u} = 0$ for uniqueness. In this case, the solution is not provided by pseudoinverse \mathbf{B}_A . However, a similar construction based on the generalized eigenvalue problem can be used instead.

Lemma 5. Let \mathbf{u} be a unique solution of $\mathbf{A} \mathbf{u} = \mathbf{P}^\top \mathbf{b}$, satisfying $\mathbf{P} \mathbf{u} = 0$ and $\Gamma \in \mathbb{R}^{n \times n}$, $\mathbf{U} \in \mathbb{R}^{n \times n-6}$ such that $\mathbf{A} \mathbf{U} = \mathbf{M} \mathbf{U} \Gamma$, $\mathbf{U}^\top \mathbf{M} \mathbf{U} = \mathbf{I}$. Then, $\mathbf{u} = \mathbf{B} \mathbf{P}^\top \mathbf{b}$, where $\mathbf{B} = \mathbf{U} \Gamma^{-1} \mathbf{U}^\top$.

Proof. First, note that the existence of matrices \mathbf{U} and Γ follows from the positive semidefiniteness of \mathbf{A} . Further, by \mathbf{M} , the orthogonality of the eigenvectors $\mathbf{M} \mathbf{U} \mathbf{x} = \mathbf{P}^\top \mathbf{b}$ holds with $\mathbf{x} = \mathbf{U}^\top \mathbf{b}$. As $\mathbf{Y}^\top \mathbf{M} \mathbf{U} = 0$, any vector $\mathbf{B} \mathbf{b}$ is \mathbf{M} orthogonal with \mathbf{Y} , and thus, $\mathbf{P} \mathbf{B} \mathbf{b} = 0$. It remains to show that the composition $\mathbf{A} \mathbf{B}$ is the identity on the subspace spanned by columns of $\mathbf{M} \mathbf{U}$. Indeed,

$$\mathbf{A} \mathbf{B} \mathbf{M} \mathbf{U} = \mathbf{A} \mathbf{U} \Gamma^{-1} \mathbf{U}^\top \mathbf{M} \mathbf{U} = \mathbf{A} \mathbf{U} \Gamma^{-1} = \mathbf{M} \mathbf{U} \Gamma^{-1} = \mathbf{M} \mathbf{U}. \quad \square$$

5 | NATURAL NORM FORMULATION

An attractive feature of the variational problem (17) is the fact that the resulting linear system is amenable to a solution by the CG method, which, when modified following Section 4, yields converging solutions. However, the projectors P' and P are only applied as a pre- and postprocessor, and the CG loop is, in this respect, detached from the continuous problem. Moreover, the method requires a special preconditioner that handles the null space of matrix \mathbf{A} . A formulation that leads to a positive definite linear system requiring only a regular (not null space aware) preconditioner shall be studied next.

Theorem 6. Let $a : V \times V \rightarrow \mathbb{R}$, $a(u, v) = 2\mu(\epsilon(u), \epsilon(v)) + \lambda(\nabla \cdot u, \nabla \cdot v)$, and let $l \in Z^0$. There exists a unique $u \in V$ satisfying

$$a(u, v) + (u_Z, v_Z) = \langle l, v \rangle \quad \forall v \in V. \quad (23)$$

Moreover, $u \in Z^\perp$.

TABLE 7 Convergence study of the natural norm formulation (23) for the singular elasticity problem from Example 2. The system is solved with relative tolerance 10^{-11} . The conjugate gradient method uses preconditioner $\text{AMG}(\mathbf{A} + \mathbf{M})$. Iteration counts are bounded in the uniform case, whereas a slight growth can be seen in the refined one. The solutions converge at an optimal rate

Size	Uniform			Size	Refined		
	$\ u - u_h\ _1$	#	$\max_Z (u_h, z) $		$\ u - u_h\ _1$	#	$\max_Z (u_h, z) $
14,739	1.03E-02 (1.14)	33	2.57E-08	13,074	3.11E-02 (0.99)	39	3.70E-08
107,811	4.84E-03 (1.09)	29	1.80E-05	98,046	1.41E-02 (1.14)	41	3.46E-08
823,875	2.36E-03 (1.03)	37	9.23E-09	759,540	6.53E-03 (1.11)	43	8.90E-08
6,440,067	1.18E-03 (1.00)	33	2.38E-05	5,978,829	3.20E-03 (1.03)	46	3.53E-08

Proof. Recall that the bilinear form above is the inner product $(u, v)_E$ from (13), which induces an equivalent norm on V (cf. Lemma 3). The existence and uniqueness of the solution now follows from the Lax–Milgram lemma. Testing the equation with $v = z \in Z$ yields $(u, z) = 0$, and in turn, $u \in Z^\perp$. \square

We remark that the solutions of (23) and (18) are equivalent because $l \in Z^0$. Note also that Theorem 4 gives equivalence bounds $(1 + C)^{-1} \|u\|_M^2 \leq \|u\|_E^2 \leq \|u\|_M^2$ for all $u \in V$ and $C = C(\Omega)$. In turn, the Riesz map with respect to the inner product $(u, v)_M = a(u, v) + (u, v)$ defines a suitable h robust preconditioner for (23). Finally, observe that the L^2 orthogonality of decomposition $u = u_Z + u_{Z^\perp}$ is respected by the inner product $(\cdot, \cdot)_E$ (see (13)). The norm $\|u\|_E$ (see (14)) thus considers Z and Z^\perp with the L^2 norm and the a induced norm, which are the natural norms for the spaces.

Using (21), the natural norm formulation (23) leads to a positive definite linear system

$$[\mathbf{A} + \mathbf{M}\mathbf{Y}(\mathbf{M}\mathbf{Y})] \mathbf{u} = \mathbf{P}^\top \mathbf{b},$$

where we recognize a dense matrix from the discretization of the \mathcal{B}_E preconditioner of the Lagrange multiplier formulation (cf. Theorem 3). Therein, the inverse of the matrix was of interest. However, relevant for the CG method here is only the matrix vector product, which can be computed efficiently by storing separately \mathbf{A} and $\mathbf{M}\mathbf{Y}$, the dual representation of rigid motions in V_h .

With (23), we finally revisit the test problem from Example 2. Results of the method are summarized in Table 7. An optimal convergence rate is observed with both uniform and nonuniform meshes. In the uniform case, the CG iteration count with the proposed Riesz map preconditioner approximated by $\text{AMG}(\mathbf{A} + \mathbf{M})$ remains bounded. There is a slight growth in the refined case. An interesting observation is the fact that the error in the orthogonality constraint is smaller in comparison to the Lagrange multiplier formulation (cf. Table 5).

6 | NEARLY INCOMPRESSIBLE MATERIALS

So far, we have assumed that μ and λ are comparable in magnitude. In this section, we handle the case where $\lambda \gg \mu$ and the material is nearly incompressible. The variational problems (6), (17), and (23) studied thus far were based on the pure displacement formulation of linear elasticity (1), and H^1 conforming finite element spaces were used for their discretization. Due to the *locking* phenomenon, the approximation properties of their respected solutions are known to degrade for nearly incompressible materials with $\lambda \gg \mu$ (equivalently, a Poisson ratio close to 1/2; see, e.g., chapter 6.3 in the work of Braess⁷). Moreover, the incompressible limit presents a difficulty for the convergence of iterative methods in the standard form.

Methods robust with respect to increasing λ can be formulated using a discretization with nonconforming elements (see chapter 11.4 in the work of Brenner and Scott⁴²). However, this method fails to satisfy Korn's inequality. To the authors' knowledge, the only primal conforming FEM that is both robust in λ and satisfies Korn's inequality is that in the works of Mardal et al.^{46,47} In addition to problems with the discretization, standard multigrid algorithms do not work well for large λ , and special-purpose algorithms must be used.⁴⁸ Related discontinuous Galerkin formulation based on $H(\text{div})$ -conforming elements is described in the work of Hong et al.,⁴⁹ where an $H(\text{div})$ multigrid method is also

introduced. For this reason, we resort to a more straightforward solution of the mixed formulation where an additional variable, the solid pressure p , is introduced. Let the solid pressure be defined as $p = \lambda \nabla \cdot u$ so that (6) is reformulated as

$$\begin{aligned} \nabla \cdot (2\mu\epsilon(u)) - \nabla p &= f && \text{in } \Omega, \\ \lambda \nabla \cdot u - p &= 0 && \text{in } \Omega, \\ \sigma(u) \cdot n &= h && \text{on } \partial\Omega. \end{aligned} \tag{24}$$

Note that the problem is singular, since any pair $z \in Z, p = 0$ can be added to the solution. In fact, such pairs constitute the kernel of (24). To obtain a unique solution, we shall, as in Section 3, require that u is orthogonal to the rigid motions Z .

Setting $Q = L^2(\Omega)$, we shall consider a variational problem for the triplet $u \in V, p \in Q, v \in Z$ such that

$$\begin{aligned} 2\mu(\epsilon(u), \epsilon(v)) + (p, \nabla \cdot v) + (v, v) &= \langle l, v \rangle && \forall v \in V, \\ (q, \nabla \cdot u) - \lambda^{-1}(p, q) &= 0 && \forall q \in Q, \\ (\eta, u) &= 0 && \forall \eta \in Z. \end{aligned} \tag{25}$$

Equation (25) defines a double-saddle-point problem

$$\mathcal{A} \begin{pmatrix} u \\ p \\ v \end{pmatrix} = \begin{pmatrix} A & B & D \\ B' & -\lambda^{-1}C & \\ D' & & \end{pmatrix} \begin{pmatrix} u \\ p \\ v \end{pmatrix} = \begin{pmatrix} l \\ 0 \\ 0 \end{pmatrix}$$

with operators $A : V \rightarrow V', B : Q \rightarrow V', C : Q \rightarrow Q'$, and $D : Z \rightarrow V'$ and functional $l : V \rightarrow \mathbb{R}$ defined as

$$\begin{aligned} \langle Au, v \rangle &= 2\mu(\epsilon(u), \epsilon(v)), && \langle Bp, v \rangle = (p, \nabla \cdot v), \\ \langle Cp, q \rangle &= (p, q), && \langle D\eta, v \rangle = (\eta, v) \end{aligned} \tag{26}$$

and

$$\langle l, v \rangle = (f, v) + (h, v)_{\partial\Omega}. \tag{27}$$

To show the well-posedness of the constrained mixed formulation (25), the abstract theory for saddle-point problems with small (note that $\lambda \gg 1$) penalty terms (see chapter 3.4 in the work of Braess⁷) is applied. To this end, we introduce the bilinear forms $a(u, v) = \langle Au, v \rangle$,

$$b(v, (p, \eta)) = \langle Bp, v \rangle + \langle D\eta, v \rangle, \tag{28}$$

$c((p, \eta), (q, \eta)) = \langle Cp, q \rangle$ so that (25) is recast as follows: Find $u \in V, (p, v) \in Q \times Z$ satisfying

$$\begin{aligned} a(u, v) + b(v, (p, v)) &= \langle l, v \rangle && \forall v \in V, \\ b(u, (q, \eta)) - \lambda^{-1}(p, q) &= 0 && \forall (q, \eta) \in Q \times Z. \end{aligned} \tag{29}$$

The space $Q \times Z$ will be considered with the norm $\|(p, \eta)\| = \sqrt{\|p\|^2 + \|\eta\|^2}$, whereas V is considered with the H^1 norm. Following theorem 4.11 in the work of Braess,⁷ problem (29) is well-posed provided that the assumptions of the Brezzi theory hold and, in addition, c is continuous and c and a are positive, that is,

$$a(u, u) \geq 0 \quad \forall u \in V \quad \text{and} \quad c((p, \eta), (p, \eta)) \geq 0 \quad \forall (p, \eta) \in Q \times Z.$$

We review that the continuity and V ellipticity of a on Z^\perp was shown in Theorem 1, and as $a(z, z) = 0, z \in Z$, the form is positive on V . Moreover, by Lemma 1 and the Cauchy-Schwarz inequality, we have that

$$b(v, (p, \eta)) = (p, \nabla \cdot v) + (v, \eta) \leq \sqrt{3}\|p\| \|\nabla v\| + \|v\| \|\eta\| \leq \sqrt{3}\sqrt{\|v\|^2 + \|\nabla v\|^2} \sqrt{\|p\|^2 + \|\eta\|^2} \leq \beta^* \|v\|_1 \|(p, \eta)\|$$

holds for any $v \in V, (p, \eta) \in Q \times Z$. It is easy to observe that the continuity and positivity of the bilinear form c hold, and thus, (29) is well-posed provided that the inf-sup condition is satisfied. We note that the proof requires extra regularity of the boundary.

Lemma 6. *Let Ω be with a smooth boundary and b be the bilinear form over $V \times (Q \times Z)$ defined in (28). There exists $\beta_* = \beta_*(\Omega)$ such that*

$$\sup_{v \in V} \frac{b(v, (p, \eta))}{\|v\|_1} \geq \beta_* \|(p, \eta)\| \quad \forall (p, \eta) \in Q \times Z.$$

Proof. Let $p \in Q$ and $\eta \in Z$ be given. Following Theorem 11.2.3 in the work of Brenner and Scott,⁴² there exists for every p a $v^* \in V$ such that

$$p = \nabla \cdot v^*, \quad (30a)$$

$$\|v^*\|_1 \leq C(\Omega)\|p\|. \quad (30b)$$

The element v^* is constructed from the unique solution of the Poisson problem, that is,

$$\begin{aligned} -\Delta w &= p && \text{in } \Omega, \\ w &= 0 && \text{on } \partial\Omega, \end{aligned} \quad (31)$$

taking $v^* = -\nabla w$. Observe that the computed $v^* \in Z^\perp$

$$-(z, v^*) = \int_{\Omega} z \nabla w = \int_{\partial\Omega} w z \cdot n - \int_{\Omega} w \nabla \cdot z = 0 \quad \forall z \in Z. \quad (32)$$

The orthogonality of v^* and (30a) yield that $b(v^* + \eta, (p, \eta)) = (p, \nabla \cdot v^*) + (\eta, \eta) = \|p\|^2 + \|\eta\|^2$. Further, by Cauchy–Schwarz and Young’s inequalities and Lemma 1, we have

$$\begin{aligned} \|v^* + \eta\|_1^2 &= \|v^* + \eta\|^2 + \|\nabla(v^* + \eta)\|^2 \\ &= \|v^*\|^2 + \|\eta\|^2 + \|\nabla v^*\|^2 + 2(\nabla v^*, \nabla \eta) + \|\nabla \eta\|^2 \\ &\leq 2\|v^*\|_1^2 + 2(\|\eta\|^2 + \|\nabla \eta\|^2) \leq 2\|v^*\|_1^2 + 2C(\Omega)\|\eta\|^2 \end{aligned}$$

so that $\|v^* + \eta\|_1 \leq c(\Omega)\|(p, \eta)\|$. Combining the observations, we obtain

$$\sup_{v \in V} \frac{b(v, (p, \eta))}{\|v\|_1} \geq \frac{b(v^* + \eta, (p, \eta))}{\|v^* + \eta\|_1} = \frac{\|p\|^2 + \|\eta\|^2}{\|v^* + \eta\|_1} \geq \frac{1}{c} \sqrt{\|p\|^2 + \|\eta\|^2} = \frac{1}{c} \|(p, \eta)\|. \quad \square$$

We remark that none of the constants of problem (29) depend on λ despite the norm of $Q \times Z$ being free of the parameter (cf. also the works of Klawonn^{50,51}). Observe also that with the H^1 norm on V , the boundedness constant of a depends on μ (cf. Theorem 1), and thus, the parameter shall be included in the norm to get a μ -independent preconditioner. This choice corresponds to considering the space V with the norm $u \mapsto \sqrt{2\mu\|\epsilon(u)\|^2 + \|u\|^2}$.

Motivated by the above, we shall consider as the preconditioner for the well-posed problem (29) a Riesz map $\mathcal{B} : (V \times Q \times Z)' \rightarrow (V \times Q \times Z)$ with respect to the inner product inducing the norm $(u, p, \eta) \mapsto \sqrt{2\mu\|\epsilon(u)\|^2 + \|u\|^2 + \|p\|^2 + \|\eta\|^2}$, that is,

$$\mathcal{B} = \begin{pmatrix} A + M & & \\ & C & \\ & & I \end{pmatrix}^{-1}, \quad (33)$$

where M and I are as defined in (13) and (11), respectively. Similar preconditioners for the Dirichlet problem have been discussed in the works of Klawonn⁵¹ and El Maliki et al.⁵²

Remark 1. (Lemma 6 in the discrete case).

The continuous inf-sup condition can be extended to the Taylor–Hood discretizations in the following way. We consider $V_h \subset V$, $Q_h \subset Q$ approximated with the lowest-order Taylor–Hood element. Given $p_h \in Q_h$, both the elements $v_h^* \in V_h$ and $w_h \in Q_h$ from Lemma 6 are found as the solution to the mixed Poisson problem

$$\begin{aligned} (v_h^*, v) + (\nabla_h w_h, v) &= 0 && \forall v \in V_h, \\ (\nabla_h q, v_h^*) &= -(p_h, q) && \forall q \in Q_h. \end{aligned}$$

The problem is well-posed due to the weak inf-sup condition

$$\sup_{v_h \in V_h} \frac{(v_h, \nabla_h q_h)}{\|v_h\|} \geq C\|q_h\|_1 \quad \forall q_h \in Q_h.$$

Since $z \in V_h$, a direct calculation shows that the orthogonality condition (32) is satisfied.

Both in the above and in the construction of the proof of Lemma 6, we relied on a well-posed mixed Poisson problem to obtain orthogonality with respect to the kernel. We note that the stable Stokes element $P_2 - P_0$ does not allow for such a construction and does not give h uniform bounds.

To show that the preconditioner (33) is robust with respect to λ , we consider (25) with $\mu = 1$ and data $h = 0$ and $f = u^*$ defined in Example 2, whereas the value of λ varies in the interval $[1, 10^{15}]$. Moreover, an exactly incompressible case shall be considered, where the operator C is set to zero.

The spaces V and Q are approximated by lowest-order Taylor–Hood elements for which the discrete inf-sup condition from Lemma 6 holds following Remark 1. As with the previous experiments, the approximate inverse of $A + M$ and C blocks are realized by a single multigrid V cycle. The final block corresponding to Z is an identity due to the employed orthonormal basis. The system is solved using the MinRes method and absolute tolerance 10^{-8} for the preconditioned residual as a convergence criterion.

From the results of the experiment, summarized in Table 8, it is evident that the iteration count is bounded in λ as well as in the discretization parameter. We note that the error in the orthogonality constraint is comparable to that reported in Table 5 for the Lagrange multiplier formulation of the pure displacement problem.

6.1 | Single–saddle-point formulation

Using formulation (29), the weak solution of (24) is computed from a double–saddle-point problem. However, if considered in $Z^\perp \times Q$, the mixed formulation of linear elasticity has just a single saddle point. A formulation that preserves this property is pursued next.

We begin by observing a few properties of the solution of the double–saddle-point problem.

Remark 2. (Properties of the solution of (29)).

(a) In the solution triplet $u \in V, p \in Q, v \in Z$, the rigid motion satisfies $(v, z) = \langle l, z \rangle$ for all $z \in Z$. In particular, $v = 0$ if and only if $l \in Z^0$. (b) The triplet u, p, v solves (29) if and only if $u, p, 0$ satisfies (29) with $l \in Z^0$.

We note that the first property follows by testing (29) with $v \in Z, p = 0$, and $\eta = 0$, whereas the second is readily checked by direct calculation. Note also that if the orthonormal basis of the space of rigid motions is employed, the Lagrange multiplier in (29) is computed simply by evaluating the right-hand side.

Due to Remark 2, it is only $u \in V$ and $p \in Q$ that are the nontrivial unknowns of the double–saddle-point problem (29). The pair can be obtained also as a solution of a system with a single saddle point.

Theorem 7. *Let $A : V \rightarrow V', B : Q \rightarrow V'$, and $C : Q \rightarrow Q'$ be the operators defined in (26) and $Y : V \rightarrow V'$ be such that $\langle Yu, v \rangle = (u_Z, v_Z)$, where $V \ni u = u_Z + u_{Z^\perp}$ and $u_Z \in Z, u_{Z^\perp} \in Z^\perp$. Then, for each $l \in V'$, there exists unique $u \in V, p \in Q$ such that*

$$A \begin{pmatrix} u \\ p \end{pmatrix} = \begin{pmatrix} A + Y & B \\ B' & -\lambda^{-1}C \end{pmatrix} \begin{pmatrix} u \\ p \end{pmatrix} = \begin{pmatrix} l \\ 0 \end{pmatrix}. \tag{34}$$

Moreover, if $l \in Z^0$, then $u \in Z^\perp$, and the triplet $u, p, 0$ is the unique solution of (29) with the right-hand side l .

Proof. We apply the results in the work of Braess⁷ (chapter 3.4 thereof) for the abstract saddle-point systems with penalty terms. To this end, we observe that operators $A + Y, B$, and C are clearly bounded on the respected spaces, whereas C is coercive on Q . The inf-sup condition for B can be verified as in the proof of Lemma 6. Indeed, let $v^* \in V$ be the element constructed in (31). Then, by (30a) and (30b), we have

$$\sup_{v \in V} \frac{\langle Bp, v \rangle}{\|v\|_1} = \sup_{v \in V} \frac{(p, \nabla \cdot v)}{\|v\|_1} \geq \frac{(p, \nabla \cdot v^*)}{\|v^*\|_1} \geq \frac{1}{C(\Omega)} \|p\|.$$

TABLE 8 Iteration counts of the preconditioned minimal residual method for the mixed linear elasticity problem (25) and different values of Lamé constant λ . The exact incompressibility case is denoted by $\lambda = \infty$. The iteration counts remain bounded for the considered values of the parameter

dim(V)	dim(Q)	λ						$\max_{Z, \lambda} (u_h, z) $
		10^0	10^4	10^8	10^{12}	10^{15}	∞	
14,739	729	81	87	88	87	88	90	9.56E–07
107,811	4,913	78	77	80	79	82	79	3.66E–06
823,875	35,937	69	72	72	72	72	72	4.02E–05
6,440,067	274,625	67	66	66	66	67	65	6.68E–05

TABLE 9 Iteration counts of the preconditioned minimal residual method for the mixed linear elasticity problem (34) and different values of Lamé constant λ . The exact incompressibility case is denoted by $\lambda = \infty$. The iteration counts remain bounded for the considered values of the parameter

dim(V)	dim(Q)	λ						$\max_{Z, \lambda} (u_h, z) $
		10^0	10^4	10^8	10^{12}	10^{15}	∞	
14,739	729	80	89	103	97	97	104	2.59E-05
107,811	4,913	60	91	94	93	93	92	8.79E-05
823,875	35,937	48	66	75	69	71	66	4.42E-04
6,440,067	274,625	36	49	50	52	50	50	5.35E-04

Next, let C_1 be the constant from Korn's inequality (5), whereas C_2 should denote the constant from inequality (9c). Using decomposition $u = u_Z + u_{Z^\perp}$ and $\|u\|_1^2 \leq 2(\|u_{Z^\perp}\|_1^2 + \|u_Z\|_1^2)$, the coercivity of $A + Y$ on V now follows

$$\begin{aligned} \langle (A + Y)u, u \rangle &= 2\mu(\epsilon(u), \epsilon(u)) + (u_Z, u_Z) = 2\mu(\epsilon(u_{Z^\perp}), \epsilon(u_{Z^\perp})) + (u_Z, u_Z) \\ &\geq 2\mu C_1 \|u_{Z^\perp}\|_1^2 + C_2^{-2} \|u_Z\|_1^2 \geq \frac{1}{2} \min(2\mu C_1, C_2^{-2}) \|u\|_1^2. \end{aligned}$$

To verify that $u \in Z^\perp$, Equation (34) is applied to the pair $z, 0$, where $z \in Z$ is arbitrary, yielding $(u_Z, z) = \langle l, z \rangle = 0$ as l is in the polar set of Z . From $u \in Z^\perp$, it follows that the last equation in (25) holds, whereas with $v = 0$, the first two equations to be satisfied by u, p are precisely (34). This verifies the final statement from the theorem. \square

Using the equivalence of norms shown in Lemma 3 and operator preconditioning, the preconditioner for the well-posed problem (34) is chosen as

$$B = \begin{pmatrix} A + M & \\ & C \end{pmatrix}^{-1} \quad (35)$$

with M defined in (13).

To show that B defines a parameter robust preconditioner for \mathcal{A} , we reuse the experimental setup from the previous section, that is, we consider (25) with $\mu = 1$, $h = 0$, and $f = u^*$ (see Example 2) and λ drawn from the interval $[1, 10^{15}]$. The operators are discretized with the $P_2 - P_1$ Taylor–Hood element that is stable for the problem following Lemma 6. Note that the discretization of operator $A + Y$ in (34) leads to a dense matrix; however, similar to Section 5, its assembly is not needed to compute the action. As with the double–saddle-point problem, the action of the discrete preconditioner is computed with AMG, whereas the system is solved with the MinRes method and absolute tolerance 10^{-8} for the preconditioned residual norm. We remark that the iterative solver uses a right-hand side orthogonalized with the discrete projector \mathbf{P}^T from (21) (cf. Theorem 7).

The results of the experiment are summarized in Table 9. We observe that with the proposed preconditioner, the iterations are bounded both in λ and the discretization parameter. The table also lists the error in the orthogonality constraint $(u_h, z) = 0 \forall z \in Z$. With the chosen convergence criterion, the error is about factor 10 larger than for the double–saddle-point formulation (cf. Table 8), whereas on the finer meshes, fewer iterations of the current solver are required for convergence.

7 | CONCLUSIONS

We have studied the singular Neumann problem of linear elasticity. Five different formulations of the problem have been analyzed, and mesh-independent preconditioners have been established for the resulting linear systems within the framework of operator preconditioning. We have proposed a preconditioner for the (singular) mixed formulation of linear elasticity, which is robust with respect to the material parameters. Using an orthonormal basis of the space of rigid motions, discrete projection operators have been derived and employed in a modification to the CG method to ensure optimal error convergence of the solution.

ACKNOWLEDGEMENTS

The authors are grateful to the anonymous referees for their constructive comments that helped significantly improve this paper. The work of Kent-Andre Mardal and Mikael Mortensen was supported by the Research Council of Norway through Center of Excellence Grant 179578 to the Center for Biomedical Computing at Simula Research Laboratory.

ORCID

Miroslav Kuchta  <http://orcid.org/0000-0002-3832-0988>

Kent-Andre Mardal  <http://orcid.org/0000-0002-4946-1110>

Mikael Mortensen  <http://orcid.org/0000-0002-3293-7573>

REFERENCES

1. Marsden JE, Hughes TJR. *Mathematical foundations of elasticity*. New York, NY: Dover Publications; 1994. Dover Civil and Mechanical Engineering Series.
2. Bauchau OA, Craig JJ. Basic equations of linear elasticity. In: *Structural analysis*. Dordrecht, The Netherlands: Springer, 2009; p. 3–51.
3. DNVGL AS. *Finite element analysis*. Høvik, Norway: Det Norske Veritas GL; 2015. Class guideline DNVGL-CG-0127.
4. Dutta-Roy T, Wittek A, Miller K. Biomechanical modelling of normal pressure hydrocephalus. *J Biomech*. 2008;41(10):2263–2271.
5. Støverud KH, Alnæs M, Langtangen HP, Haughton V, Mardal K-A. Poro-elastic modeling of Syringomyelia - a systematic study of the effects of pia mater, central canal, median fissure, white and gray matter on pressure wave propagation and fluid movement within the cervical spinal cord. *Comput Methods Biomech Biomed Engin*. 2016;19(6):686–698.
6. Tobie G, Čadež O, Sotin C. Solid tidal friction above a liquid water reservoir as the origin of the south pole hotspot on Enceladus. *Icarus*. 2008;196(2):642–652. Mars Polar Science IV.
7. Braess D. *Finite elements: theory, fast solvers, and applications in solid mechanics*. Cambridge, UK: Cambridge University Press; 2001.
8. Ruge JW, Stüben K. Algebraic multigrid. In: *Multigrid methods*. Philadelphia, PA: Society for Industrial and Applied Mathematics; 1987.
9. Baker AH, Kolev TV, Yang UM. Improving algebraic multigrid interpolation operators for linear elasticity problems. *Numer Linear Algebra Appl*. 2010;17(2–3):495–517.
10. Griebel M, Oeltz D, Schweitzer MA. An algebraic multigrid method for linear elasticity. *SIAM J Sci Comput*. 2003;25(2):385–407.
11. Vassilevski PS, Zikatanov LT. Multiple vector preserving interpolation mappings in algebraic multigrid. *SIAM J Matrix Anal Appl*. 2006;27(4):1040–1055.
12. Vaněk P, Mandel J, Brezina M. Algebraic multigrid by smoothed aggregation for second and fourth order elliptic problems. *Computing*. 1996;56(3):179–196.
13. Mandel J, Brezina M, Vaněk P. Energy optimization of algebraic multigrid bases. *Computing*. 1999;62(3):205–228.
14. Brezina M, Cleary AJ, Falgout RD, et al. Algebraic multigrid based on element interpolation (AMGe). *SIAM J Sci Comput*. 2001;22(5):1570–1592.
15. Jones JE, Vassilevski PS. AMGe based on element agglomeration. *SIAM J Sci Comput*. 2001;23(1):109–133.
16. Henson VE, Vassilevski PS. Element-free AMGe: general algorithms for computing interpolation weights in AMG. *SIAM J Sci Comput*. 2001;23(2):629–650.
17. Kraus JK. Algebraic multigrid based on computational molecules, 2: linear elasticity problems. *SIAM J Sci Comput*. 2008;30(1):505–524.
18. Karer E, Kraus JK. Algebraic multigrid for finite element elasticity equations: determination of nodal dependence via edge-matrices and two-level convergence. *Int J Numer Methods Eng*. 2010;83(5):642–670.
19. Farhat C, Roux F-X. A method of finite element tearing and interconnecting and its parallel solution algorithm. *Int J Numer Methods Eng*. 1991;32(6):1205–1227.
20. Balay S, Brown J, Buschelman K, et al. *PETSc users manual*. Lemont, IL: Argonne National Laboratory; 2013. ANL-95/11 - Revision 3.4.
21. Falgout RD, Jones JE, Yang UM. The design and implementation of hypre, a library of parallel high performance preconditioners. In: *Numerical solution of partial differential equations on parallel computers*. Berlin, Germany: Springer, 2006; p. 267–294. Lecture Notes in Computational Science and Engineering, No. 51.
22. Brezina M, Falgout R, MacLachlan S, Manteuffel T, McCormick S, Ruge J. Adaptive algebraic multigrid. *SIAM J Sci Comput*. 2006;27(4):1261–1286.
23. Brezina M, Falgout R, MacLachlan S, Manteuffel T, McCormick S, Ruge J. Adaptive smoothed aggregation (α SA) multigrid. *SIAM Rev*. 2005;47(2):317–346.
24. Mardal K-A, Winther R. Preconditioning discretizations of systems of partial differential equations. *Numer Linear Algebra Appl*. 2011;18(1):1–40.
25. Ciarlet PG. On Korn's inequality. *Chin Ann Math Ser B*. 2010;31(5):607–618.
26. Bochev P, Lehoucq RB. On the finite element solution of the pure Neumann problem. *SIAM Rev*. 2005;47(1):50–66.
27. Logg A, Mardal KA, Wells GN. *Automated solution of differential equations by the finite element method: the FEniCS book*. Vol. 84. Berlin, Germany: Springer-Verlag Berlin Heidelberg; 2012.

28. Vanek P, Brezina M, Tezaur R. Two-grid method for linear elasticity on unstructured meshes. *SIAM J Sci Comput.* 1999;21(3):900–923.
29. Brezzi F. On the existence, uniqueness and approximation of saddle-point problems arising from Lagrangian multipliers. *Rev Française Automat Informat Recherche Opérationnelle Sér Rouge.* 1974;8(R-2):129–151.
30. Fortin M. An analysis of the convergence of mixed finite element methods. *RAIRO Anal Numér.* 1977;11(4):341–354.
31. Arnold DN, Brezzi F, Fortin M. A stable finite element for the Stokes equations. *Calcolo.* 1984;21(4):337–344.
32. Málek J, Strakoš Z. Preconditioning and the conjugate gradient method in the context of solving PDEs. Philadelphia, PA: Society for Industrial and Applied Mathematics; 2014.
33. Kuchta M, Mardal KA, Mortensen M. Characterisation of the space of rigid motions in arbitrary domains. In: Proceedings of 8th National Conference on Computational Mechanics; 2015; Barcelona, Spain. Barcelona, Spain: International Centre for Numerical Methods in Engineering; 2015.
34. Gurtin ME. An introduction to continuum mechanics. New York, NY: Academic Press, Inc; 1982. Mathematics in science and engineering.
35. Bergh J, Löfström J. Interpolation spaces: an introduction. Berlin, Germany: Springer-Verlag Berlin Heidelberg; 1976. Grundlehren der mathematischen Wissenschaften.
36. Benzi M, Golub GH, Liesen J. Numerical solution of saddle point problems. *Acta Numer.* 2005;14:1–137.
37. Paige CC, Saunders MA. Solution of sparse indefinite systems of linear equations. *SIAM J Numer Anal.* 1975;12(4):617–629.
38. Mardal K-A, Haga JB. Block preconditioning of systems of PDEs. In: Logg A, Mardal K-A, Wells G, editors. Automated solution of differential equations by the finite element method: the FEniCS book. Berlin, Germany: Springer-Verlag Berlin Heidelberg; 2012.
39. Greenbaum A. Iterative methods for solving linear systems. Philadelphia, PA: Society for Industrial and Applied Mathematics; 1997. Frontiers in applied mathematics.
40. Liesen J, Tichý P. Convergence analysis of Krylov subspace methods. *GAMM Mitt Ges Angew Math Mech.* 2004;27(2):153–173.
41. Trefethen LN, Bau D. Numerical linear algebra. Philadelphia, PA: Society for Industrial and Applied Mathematics; 1997.
42. Brenner S, Scott R. The mathematical theory of finite element methods. New York, NY: Springer; 2007. Texts in applied mathematics.
43. Penrose R. A generalized inverse for matrices. *Math Proc Cambridge Philos Soc.* 2008;51(3):406–413.
44. Lanczos C. Linear differential operators. Philadelphia, PA: Society for Industrial and Applied Mathematics; 1997. Classics in applied mathematics.
45. Shewchuk JR. An introduction to the conjugate gradient method without the agonizing pain. Pittsburgh, PA: Carnegie Mellon University; 1994. Technical report.
46. Mardal KA, Tai X-C, Winther R. A robust finite element method for Darcy–Stokes flow. *SIAM J Numer Anal.* 2002;40(5):1605–1631.
47. Mardal K-A, Winther R. An observation on Korn's inequality for nonconforming finite element methods. *Math Comput.* 2006;75(253):1–6.
48. Schöberl J. Multigrid methods for a parameter dependent problem in primal variables. *Numer Math.* 1999;84(1):97–119.
49. Hong Q, Kraus J, Xu J, Zikatanov L. A robust multigrid method for discontinuous Galerkin discretizations of Stokes and linear elasticity equations. *Numer Math.* 2016;132(1):23–49.
50. Klawonn A. Block-triangular preconditioners for saddle point problems with a penalty term. *SIAM J Sci Comput.* 1998;19(1):172–184.
51. Klawonn A. An optimal preconditioner for a class of saddle point problems with a penalty term. *SIAM J Sci Comput.* 1998;19(2):540–552.
52. El Maliki A, Fortin M, Tardieu N, Fortin A. Iterative solvers for 3D linear and nonlinear elasticity problems: displacement and mixed formulations. *Int J Numer Methods Eng.* 2010;83(13):1780–1802.

How to cite this article: Kuchta M, Mardal K-A, Mortensen M. On the singular Neumann problem in linear elasticity. *Numer Linear Algebra Appl.* 2019;26:e2212. <https://doi.org/10.1002/nla.2212>

APPENDIX

EIGENVALUE BOUNDS FOR LAGRANGE MULTIPLIER PRECONDITIONERS

Bounds for the eigenvalues of operators $\mathcal{B}_E \mathcal{A}$ and $\mathcal{B}_M \mathcal{A}$ from (7) and (16) are approximated by considering the eigenvalue problems

$$\begin{pmatrix} \mathbf{A} & \mathbf{B} \\ \mathbf{B}^\top & \mathbf{0} \end{pmatrix} \begin{pmatrix} \mathbf{u} \\ \mathbf{p} \end{pmatrix} = \lambda \mathbf{B}_i^{-1} \begin{pmatrix} \mathbf{u} \\ \mathbf{p} \end{pmatrix} \quad (\text{A1})$$

with the left-hand side as the discretization of (7) and \mathbf{B}_i , $i \in \{E, M\}$ as discretizations of preconditioners \mathcal{B}_i from (16). The spectrum of the symmetric, indefinite problem (A1) is a union of negative and positive intervals $[\lambda_{\min}^-, \lambda_{\max}^-]$ and $[\lambda_{\min}^+, \lambda_{\max}^+]$. Following the analysis in Theorems 3 and 4, negative bounds equal to -1 are expected for both

TABLE A1 Spectral bounds for eigenvalue problems (A1). (Top) The body is a cube. (Bottom) The body is a cylinder

	Size	κ	$\lambda_{\min}^- + 1$	$\lambda_{\max}^- + 1$	$\lambda_{\min}^+ - 1$	$\lambda_{\max}^+ - 1$
\mathcal{B}_E	87	1.0000	$-6.83E-11$	$2.92E-11$	$-4.36E-11$	$5.89E-12$
	381	1.0000	$-1.38E-10$	$7.00E-12$	$-1.61E-10$	$5.55E-15$
	2,193	1.0000	$-5.88E-10$	$1.65E-11$	$-6.23E-10$	$9.55E-15$
	14,745	1.0000	$-1.10E-08$	$-4.27E-09$	$-2.00E-08$	$1.73E-14$
\mathcal{B}_M	87	1.0001	$-6.64E-11$	$4.46E-12$	$-1.10E-04$	$1.03E-11$
	381	1.0002	$-1.35E-10$	$-1.06E-11$	$-2.33E-04$	$-5.33E-12$
	2,193	1.0004	$-5.73E-10$	$-1.12E-11$	$-4.00E-04$	$5.91E-12$
	14,745	1.0005	$-2.37E-09$	$-7.73E-11$	$-4.97E-04$	$-4.47E-11$
\mathcal{B}_E	210	1.0000	$-3.91E-12$	$-4.46E-13$	$-4.58E-12$	$9.33E-15$
	462	1.0000	$-3.82E-12$	$-8.91E-13$	$-4.55E-12$	$5.77E-15$
	1,764	1.0000	$-9.32E-12$	$-4.40E-12$	$-1.08E-11$	$1.31E-14$
	8,292	1.0000	$-3.71E-11$	$-1.74E-11$	$-4.06E-11$	$6.26E-14$
\mathcal{B}_M	210	1.0752	$1.84E-02$	$7.00E-02$	$-7.00E-02$	$-2.57E-06$
	462	1.0219	$1.94E-03$	$2.14E-02$	$-2.14E-02$	$-2.21E-06$
	1,764	1.0069	$1.14E-03$	$6.82E-03$	$-6.82E-03$	$-4.57E-07$
	8,292	1.0022	$1.60E-04$	$1.66E-03$	$-2.17E-03$	$-2.10E-08$

preconditioners. Further, the positive eigenvalues are bounded from above by 1. Finally, $\lambda_{\min}^+ = -1$ for \mathcal{B}_E , whereas the constant $C = C(\Omega)$ from Korn's inequality determines the bound for \mathcal{B}_M .

In the experiment, Ω as a cube from Example 2 and a hollow cylinder with inner and outer radii $\frac{1}{2}$, 1 and height 2 are considered. Lamé constants $\mu = 384$ and $\lambda = 577$ are used. For both bodies, $C \approx 1$ is observed (cf. Table A1). The remaining bounds agree well with the analysis.